

Efficient distributional regression trees learning algorithms for calibrated non-parametric probabilistic forecasts

Quentin Duchemin*[&] Guillaume Obozinski[†]

Abstract

The perspective of developing trustworthy AI for critical applications in science and engineering requires machine learning techniques that are capable of estimating their *own uncertainty*. In the context of regression, instead of estimating a conditional mean, this can be achieved by producing a predictive interval for the output, or to even learn a model of the conditional probability $p(y|x)$ of an output y given input features x . While this can be done under parametric assumptions with, e.g. generalized linear model, these are typically too strong, and non-parametric models offer flexible alternatives. In particular, for scalar outputs, learning directly a model of the *conditional cumulative distribution function* of y given x can lead to more precise probabilistic estimates, and the use of proper scoring rules such as the *weighted interval score* (WIS) and the *continuous ranked probability score* (CRPS) lead to better coverage and calibration properties.

This paper introduces novel algorithms for learning probabilistic regression trees for the WIS or CRPS loss functions. These algorithms are made computationally efficient thanks to an appropriate use of known data structures - namely *min-max heaps*, *weight-balanced binary trees* and *Fenwick trees*.

Through numerical experiments, we demonstrate that the performance of our methods is competitive with alternative approaches. Additionally, our methods benefit from the inherent interpretability and explainability of trees. As a by-product, we show how our trees can be used in the context of conformal prediction and explain why they are particularly well-suited for achieving *group-conditional coverage guarantees*.

1 Introduction

Unlike standard regression methods which target the conditional mean of the response to explanatory variables, distributional regression aims at estimating the entire conditional distribution of the outcome. Distributional regression is becoming more and more popular since understanding variability and uncertainty is crucial in fields like econometrics, climatology, and biostatistics. [RS05] laid foundational work with their generalized additive models for location, scale, and shape, in which a parametric distribution is assumed for the response variable but the parameters of this distribution can vary according to explanatory variables using linear, nonlinear or smooth functions. Another line of work relies on density estimation techniques to learn the conditional distributions with methods ranging from mixture models [GL07] to Bayesian ones [DPP07]. More recently, the deep learning area gave birth to generative models achieving remarkable results, especially in the field of imaging [RBL⁺22]. These generative models aim at learning to sample from the training data distribution via a transformation of a simple distribution. One can mention normalizing flows [KPB20] or diffusion models [HJA20]. These methods have been widely applied to images and text, but recent works [SM24] adapt these methods to classical regression. We refer to a recent review of distributional regression approaches in [KSS23].

While distributional regression provides a comprehensive view of the response distribution, there are cases where practitioners are interested in specific aspects of this distribution, rather than the entire probability landscape. For instance, understanding the behavior of a response variable at its extremes or at specific percentiles can be crucial for applications such as risk assessment or resource allocation. This is where quantile regression [KBJ78, Reg17] becomes a powerful complementary tool. Quantile

*Swiss Data Science Center, EPFL & ETH Zürich, Switzerland, quentin.duchemin@epfl.ch

[†]Swiss Data Science Center, EPFL & ETH Zürich, Switzerland, guillaume.obozinski@epfl.ch

regression has become a standard technique and is usually achieved by minimizing the so-called pinball loss. The pinball loss ℓ_τ for the quantile of level $\tau \in (0, 1)$ is defined by

$$\ell_\tau(\xi) = (\tau - \mathbb{1}_{\xi < 0})\xi, \quad \xi \in \mathbb{R}$$

and is such that

$$q_\tau(x) \in \arg \min_{q \in \mathbb{R}} \mathbb{E}_P[\ell_\tau(Y - q) \mid X = x],$$

where $q_\tau(x)$ is the quantile of level τ of the distribution of Y conditional on $X = x$. While the pinball loss is not differentiable at zero, optimization can still be performed using subgradient methods or by employing a smoothed approximation, such as the Huber loss for the median. This approach enables the use of standard regression models to estimate specific conditional quantiles of interest. Notable examples include the use of neural networks [Can11], kernel methods [TLSS06], Gaussian processes [AR15] or splines [TCM⁺10]. We refer to the survey paper [TPFG20] for a more exhaustive list of quantile regression methods.

Simultaneous multiple quantile regression provides a natural bridge between full distributional regression and single quantile regression. Estimating a large set of quantiles rather than a single one can be important in various applications such as decision making [HV99], personalized health [KS22] or finance [EM04] where professionals often need to understand the potential losses or gains at various quantiles to assess the risk of different investments or portfolios. A straightforward approach to multiple quantile regression involves fitting separate models for each quantile of interest. However, this method can be suboptimal in practice, as it fails to leverage the shared information between the models, potentially leading to poorer performance. Additionally, it may result in the undesirable phenomenon of quantile crossing, where estimated quantiles are inconsistent, namely when higher quantiles are lower than lower quantiles. To address these issues, regularized approaches [ZY08] or constrained methods [LW09] have been proposed to couple different quantile models. To improve computational efficiency, a promising strategy is to optimize the sum of pinball losses across multiple quantiles in a single model [JOM⁺16], rather than fitting separate models for each quantile. The sum of pinball losses is known as the weighted interval score (WIS) in the probabilistic forecasting community [BRGR21]. Given M quantile levels $0 < \tau_1 < \dots < \tau_M < 1/2$, the WIS loss is defined by:

$$\ell_{WIS(\tau_{1:M})}(\{q_{\tau_m}\}_{m=1}^{2M+1}, y) = \frac{2}{2M+1} \sum_{m=1}^{2M+1} \ell_{\tau_m}(y - q_{\tau_m}),$$

where $\tau_{M+1} = 1/2$ and where $\tau_{M+2} = 1 - \tau_M, \dots, \tau_{2M+1} = 1 - \tau_1$. The WIS is primarily a loss function on quantiles, but can actually be interpreted as a loss function over a cumulative distribution function F writing

$$\ell_{WIS(\tau_{1:M})}(F, y) = \frac{2}{2M+1} \sum_{m=1}^{2M+1} \ell_{\tau_m}(y - F^{-1}(\tau_m)).$$

By increasing the number of quantiles considered, one intuitively expects the WIS loss to be sensitive to any change in the cumulative distribution function F . This intuition can be formalized, as shown in [BG21], by proving that the WIS loss asymptotically converges to the continuous ranked probability score (CRPS) as $M \rightarrow \infty$:

$$\text{CRPS}(F, y) := \int_{-\infty}^{+\infty} (F(s) - \mathbb{1}_{s \geq y})^2 ds.$$

The CRPS is a metric designed to evaluate the accuracy of probabilistic predictions. This convergence bridges the gap between quantile-based evaluation and full distributional assessment.

While the CRPS and WIS losses are appealing for training better-calibrated probabilistic forecasters, their adoption in practice remains limited due to several challenges. Firstly, optimizing the risk associated to the CRPS loss can be computationally challenging since explicit solutions are only available for limited parametric cases [JKL17] and gradients of the CRPS might be tractable under some strong assumption on the data distribution [CC21]. Secondly, most existing methods for minimizing the risk associated to the WIS loss require either adding constraints during training or implementing post-processing adjustments to enforce non-crossing quantiles. These additional procedures not only complicate the optimization process but might also negatively impact overall model performance.

Thirdly, and perhaps most critically, many of the recent deep learning-based methods for distributional learning, while powerful, suffer from a lack of interpretability. This is a significant drawback in high-stakes applications, such as the medical field, where understanding model decisions is crucial for trust and accountability. There is, therefore, a growing need for interpretable models that can optimize CRPS or WIS losses while maintaining strong predictive performance and computational efficiency.

Among interpretable models, one of the most popular is regression trees. This can be attributed to their intuitive representation of decision-making processes, which appeals to both experts and non-experts. Additionally, their versatility in handling diverse data types renders them applicable from finance to healthcare, image recognition, or natural language processing. The construction of decision trees entails an iterative process of selecting features to split the dataset, guided by an entropy to quantify the impurity or disorder within nodes. At each node, the algorithm assesses potential splitting thresholds for each feature, choosing the one that minimizes overall impurity. The choice of splitting criteria, namely the choice of the impurity measure, is pivotal in optimizing the tree's ability to capture patterns and make accurate predictions. Most common impurity measures can be expressed as the empirical risk of a corresponding loss function ℓ , for the optimal value of leaf parameters. These impurity measures can therefore be seen as a generalized form of entropy H_ℓ associated with the loss function ℓ ,

$$\mathbb{H}_\ell(P) := \inf_a \mathbb{E}_P[\ell(a, Y)]. \quad (1)$$

This connection is well-known in the literature [DeG62, Eq.(2.14)], [GD04, Xu20]. The entropy associated with a specific loss function is also referred to as the generalized entropy or the Bayes risk [Xu20, BS21]. In both classification and regression settings, the range of entropies employed for training decision trees remains relatively limited. In binary classification, the usual choices for entropy include the Gini entropy, the Shannon entropy, or the 0-1 entropy (cf. [MSP22]) corresponding respectively to the squared loss, the log loss and the 0-1 loss. For regression, common practice involves opting for a splitting criterion based on the squared loss or the absolute error.

In this work, we present two novel algorithms for efficiently training distributional regression trees for the WIS loss and the CRPS loss.

Related work. As far as we know, there are two ways to learn a conditional quantile model using regression trees in the current literature:

- Either one uses the so-called Quantile Regression Forest method [MR06]. This method, by using the squared loss, benefits from well-established and optimized packages for training regression trees. Additionally, these trees can be used to estimate quantiles of any level with the resulting quantiles guaranteed to be non-crossing (cf. [RPC19, Section 6]). However, a key drawback is that the splitting criterion used to construct the tree is well adapted to capture the fluctuations of the conditional mean but not the conditional quantiles of interest, which potentially decreases statistical efficiency.
- [BKV15] considers the problem of learning a single conditional quantile model using a single quantile regression trees trained with the quantile loss function, also known as the pinball loss. The entropy associated to the pinball loss is

$$\begin{aligned} \mathbb{H}_{\ell_\tau}(P) &= \min_{q \in \mathbb{R}} \mathbb{E}_P[\ell_\tau(Y - q)] \\ &= (1 - \tau)\mathbb{E}_P[(q - Y)_+] + \tau\mathbb{E}_P[(Y - q)_+], \end{aligned}$$

where for any real number x , $(x)_+ = \max(x, 0)$. In the empirical setting where we have observations $\mathbf{y} = \{y_i\}_{i=1}^n$ sampled from P , the empirical entropy is

$$H_{\ell_\tau}(\mathbf{y}) := \min_{q \in \mathbb{R}} \frac{1}{n} \sum_{i=1}^n \ell_\tau(y_i - q) = \frac{1}{n} \sum_{i=1}^n \ell_\tau(y_i - \hat{q}_\tau), \quad (2)$$

where $\hat{q}_\tau = y_{(\lceil \tau n \rceil)}$ is the empirical quantile of level τ of the sequence $\mathbf{y} = (y_i)_{i=1}^n$. The tree is then trained using the standard CART algorithm [Bre17] with the entropy from Eq.(2): at each node, the data is split by selecting the feature and the threshold that minimize the entropy within the resulting subsets. This process iteratively creates nodes that represent the most homogeneous

possible groups by reducing overall entropy. The procedure to find the data split maximizing the information gain defined with the entropy from Eq.(2) at a given node of the tree with n samples and d features has a time complexity of order $\mathcal{O}(dn \log n)$ (cf. [BKV15]).

In this paper, we complement the work of [BKV15] by presenting two efficient algorithms to learn distributional regression trees for the WIS and CRPS losses.

Outline. In this work, we first introduce two novel algorithms to learn distributional regression trees (Sec. 2): the first minimizes the empirical entropy associated to the WIS loss, which we call Pinball Multiple Quantiles Regression Trees (PMQRT); the second algorithm learns distributional regression trees (CRPS-RT) for the CRPS loss. To improve the latter algorithm, we propose to use an unbiased estimate of the CRPS risk using leave-one-out without additional computational cost (Sec. 2.4). Detailed descriptions of the algorithms can be found in Section B. In Section 3, we evaluate the empirical performance of random forests of PMQRTs (PMQRF) and CRPS-RTs (CRPS-RF) through a series of experiments. We demonstrate the scalability of the proposed algorithms and that by using a CRPS-RF, we can develop a non-parametric method for learning conditional distribution functions that rivals existing approaches.

2 Learning distributional regression trees

This section introduces algorithms designed to construct regression trees with common splits for modeling multiple quantiles or the entire conditional distribution. Unlike traditional approaches that treat different quantiles independently, our methods seek to identify shared split points to improve interpretability and computational efficiency. We propose two tree-learning algorithms tailored to distinct loss functions: one for the WIS and another for the CRPS. The following subsections outline these methods and address the challenges inherent in optimizing these distinct objectives.

2.1 Notations

To evaluate potential splits based on a single feature, the vector of output values must first be sorted by increasing order of that input feature. For each possible split index s , we then consider the subset of output values corresponding to the first s elements of the sorted sequence and compute an empirical quantile - that is, an order statistic - of these labels. This motivates the introduction of the following notations: Let us consider an arbitrary sequence $\mathbf{a} = (a_1, \dots, a_n)$ of real values of size n . For any $s \in [n]$, we denote by $\mathbf{a}^{(s)} := (a_1, \dots, a_s)$ the prefix sequence of \mathbf{a} . For any $s \in [n]$, $a_{(s)}$ corresponds to the s -th largest value of the sequence \mathbf{a} , while for any $i \in [s]$, $a_{(i)}^{(s)}$ refers to the i -th largest value of the prefix sequence $\mathbf{a}^{(s)}$.

2.2 Pinball multi-quantile regression tree

Extracting multiple quantiles from a single tree. When estimating multiple quantiles at different levels, one option is to use Quantile Regression Forests (QRF), where the set of trained trees can be queried to estimate any quantile. However, as noted earlier, these trees are learned using the square loss and aim to predict the conditional mean of the data distribution, which may result in suboptimal estimates for the quantiles.

A simple alternative consists of relying on a set of trees, each targeting a specific quantile level τ and learned following the method from [BKV15] to minimize the entropy associated with the pinball loss ℓ_τ . This approach has two main limitations. First, we lose the guarantee of non-crossing quantiles, which holds in the QRF method. Second, each learned tree forms its own partition of the feature space based on the quantile level it is targeting. This not only hampers the application of these trees for tasks such as group conformal prediction (cf. Section 3.4), but it may also lead to reduced statistical efficiency due to the lack of a unified feature space partitioning and the potential increase in the variance of the quantile estimates.

To bypass these limitations, we present an approach that takes the best of the ones above-mentioned. We propose learning a tree that produces all conditional quantiles estimates in each

leaf and that most importantly relies on a common split for all quantiles considering the sum of pinball losses $\ell_{\tau_1, \dots, \tau_m}$ defined for any $\boldsymbol{\tau}, \mathbf{q} \in \mathbb{R}^M$ as

$$\ell_{\tau_1, \dots, \tau_m}(\mathbf{q}, y) := \sum_{m=1}^M \ell_{\tau_m}(y - q_m).$$

The multi-dimensional optimization problem over $\mathbf{q} \in \mathbb{R}^M$ that defines the empirical entropy associated with $\ell_{\tau_1, \dots, \tau_m}$ is separable, which leads to

$$H_{\ell_{\tau_1, \dots, \tau_m}}(\mathbf{y}) = \sum_{m=1}^M H_{\ell_{\tau_m}}(\mathbf{y}). \quad (3)$$

Relying on the CART algorithm, training a regression tree considering the loss $\ell_{\tau_1, \dots, \tau_m}$ requires to compute the entropies $H_{\ell_{\tau_1, \dots, \tau_m}}(\mathbf{y}^{(s)})$ associated to any prefix sequence $\mathbf{y}^{(s)} := (y_1, \dots, y_s)$ from a given sequence of values $\mathbf{y} = (y_1, \dots, y_n)$. We end up with a problem similar to [BKV15] but with multiple quantiles at the same time.

Efficient pinball loss node splitting with max heaps. The algorithm proposed in [BKV15] for learning a quantile regression tree that minimizes the empirical entropy associated with a single pinball loss ℓ_{τ} uses two heaps (cf. [HH13]). At a given node in the tree, with data $\{(\mathbf{x}_i, y_i)\}_{i=1}^n$, the goal is to find the threshold that provides the best information gain using the entropy from Eq.(2) for each feature j . Assuming without loss of generality that $x_{i,j} \leq \dots \leq x_{n,j}$ for some feature j , identifying the optimal threshold reduces to computing the entropies for all prefix and suffix sequences of \mathbf{y} . Since the suffix sequences of \mathbf{y} correspond to prefix sequences of $(y_{(n)}, \dots, y_{(1)})$, it is sufficient to explain how [BKV15] computes efficiently the entropies of the sequences $\mathbf{y}^{(s)}$ for all $s \in [n]$. As shown in [BKV15, Sec.III.B], the entropy $H_{\ell_{\tau}}(\mathbf{a})$ for any nondecreasing sequence \mathbf{a} of length s can be computed in $\mathcal{O}(1)$ time using $a_{\lceil \tau(s-1) \rceil}$, $a_{\lceil \tau s \rceil}$, $\sum_{i=1}^{\lceil \tau(s-1) \rceil} a_i$, and $\sum_{i=1}^s a_i$. The authors show that these quantities can be efficiently tracked by initializing two empty heaps - one max-heap \mathcal{H}_{low} and one min-heap \mathcal{H}_{high} - and by sequentially adding elements y_s from $s = 1$ to n to them. At each step s , the update of the two heaps ensures that \mathcal{H}_{low} contains all elements $(y_{(1)}, \dots, y_{(\lceil \tau(s-1) \rceil)})$ and \mathcal{H}_{high} contains all elements $(y_{(\lceil \tau s \rceil)}, \dots, y_{(s)})$. Querying the maximum value in \mathcal{H}_{low} and the minimum value in \mathcal{H}_{high} can be done in constant time while the heaps update require $\mathcal{O}(\log(s))$ time.

From Eq. (3), the empirical entropy of a sum of pinball losses $\ell_{\tau_1, \dots, \tau_M}$ is the sum of the empirical entropies for each individual pinball loss. As a consequence, a straightforward approach to estimate quantiles at multiple levels using a single tree is to apply the method from [BKV15] independently for each quantile level. However, this brute-force approach incurs a space complexity of $\mathcal{O}(Mn)$, making it inefficient as the number of quantile levels M increases.

To address this limitation, we propose a new algorithm whose space complexity remains of the order of the size of the dataset, regardless of the number of estimated quantiles.

Efficient pinball multi-quantile loss node splitting with a set of min-max heaps. Using the decomposition Eq. (3), one can deduce from [BKV15] that the empirical entropy $H_{\ell_{\tau_1, \dots, \tau_m}}(\mathbf{y}^{(s)})$ of any prefix sequence $\mathbf{y}^{(s)}$ can be obtained by keeping track of *i*) the empirical quantiles $\hat{q}_{\tau_1}, \dots, \hat{q}_{\tau_M}$ of level τ_1, \dots, τ_M of $\mathbf{y}^{(s)}$ and *ii*) of the cumulative sums $\left(\sum_{i \leq \lceil \tau_m s \rceil} y_{(i)}^{(s)}\right)_{m=1}^M$ and $\sum_{i \leq s} y_{(i)}^{(s)}$. We propose an efficient algorithm to keep track of these quantities relying on $M + 1$ min-max heaps: $\mathcal{H}_1, \dots, \mathcal{H}_M, \mathcal{H}_{M+1}$. Let us recall that a min-max heap is a variant of a binary heap allowing for constant-time access to both the minimum and maximum elements. On even levels, the heap adheres to min-heap properties, while odd levels follow max-heap properties. This ensures that the root always holds the minimum, and its children represent the maximum elements. Insertions and deletions have logarithmic time complexity, providing a balance between efficient extremal element access and effective heap modification. As for standard regression trees, we increase the index s from 1 to n to cover all the prefix sequences $\mathbf{y}^{(s)}$ of interest to determine the position of the split at the current node. The $M + 1$ min-max heaps are updated at each iteration s to ensure that \mathcal{H}_1 contains all the elements $\{y_{(1)}^{(s)}, \dots, y_{(\lceil \tau_1 s \rceil)}^{(s)}\}$, \mathcal{H}_2 contains all the elements $\{y_{(\lceil \tau_1 s \rceil + 1)}^{(s)}, \dots, y_{(\lceil \tau_2 s \rceil)}^{(s)}\}$, \dots , \mathcal{H}_M contains all the elements $\{y_{(\lceil \tau_{M-1} s \rceil + 1)}^{(s)}, \dots, y_{(\lceil \tau_M s \rceil)}^{(s)}\}$, and \mathcal{H}_{M+1} contains all the elements $\{y_{(\lceil \tau_M s \rceil + 1)}^{(s)}, \dots, y_{(s)}^{(s)}\}$.

Querying the quantile of level τ_m simply involves accessing the maximum of the heap \mathcal{H}_m , or the minimum of the heap \mathcal{H}_j for $j := \arg \min\{i > m \mid \mathcal{H}_i \neq \emptyset\}$ in case \mathcal{H}_m is empty. Our min-max heap structures are also designed to store the total sums of elements in each heap, facilitating access to cumulative sums of the form $\sum_{i \leq \lceil \tau_m s \rceil} y_{(i)}^{(s)}$ in $\mathcal{O}(m)$ time by querying the total sums of heaps \mathcal{H}_1 to \mathcal{H}_m . Overall, the worst time complexity for a node split with n data points and d features is $\mathcal{O}(Mdn \log n)$ as illustrated in Table 1. The detailed algorithm can be found in Section B.1.

2.3 CRPS distributional regression tree

In the previous section, we presented a computationally efficient method for learning a Pinball multi-quantile regression tree. Such a tree has the advantage of leveraging information from different parts of the conditional distribution to build the partition, ensuring non-crossing quantile estimates, and offering a flexible tool for modern uncertainty quantification, ideal for applications such as group conformal methods, see Section 3.4. However, a Pinball multi-quantile regression tree focuses only on specific quantiles, limiting its ability to represent the full conditional distribution. As a result, it may overlook key aspects of the data distribution, affecting predictive accuracy. Furthermore, certain methods, such as the distributional conformal prediction method proposed in [CWZ21], require querying quantiles at arbitrary levels, and constraining the model to a fixed set of predefined quantiles may hinder its effectiveness.

To bypass these limitations, we propose to learn trees that minimize the empirical entropy associated with the Continuous Ranked Probability Score (CRPS), namely

$$H_{\text{CRPS}}(\mathbf{y}) := \min_F \frac{1}{n} \sum_{i=1}^n \text{CRPS}(F, y_i) = \frac{1}{n} \sum_{i=1}^n \text{CRPS}(\hat{F}_n, y_i), \quad (4)$$

where \hat{F}_n is the empirical CDF of the observed data \mathbf{y} . The CRPS is a strictly proper scoring rule, as detailed in [GR07], incentivizing forecasters to provide accurate and well-calibrated uncertainty estimates, making it a valuable tool in probabilistic forecasting evaluations.

CRPS-Based tree training: Theoretical foundations and design. To construct a distributional regression tree based on the generalized entropy induced by the CRPS loss, one must identify the split at a given leaf that results in the largest impurity gain. Given a leaf with data $\{(\mathbf{x}_i, y_i)\}_{i=1}^n$, this process involves computing the entropies for every feature j using every prefix sequence $\mathbf{y}^{(s)} = \{y_1, \dots, y_s\}$ and every suffix sequence (y_{s+1}, \dots, y_n) of the data sequence \mathbf{y} , assuming for simplicity that $x_{1,j} \leq \dots \leq x_{n,j}$. Relying on the entropy expression from Eq. (4), this requires constructing the empirical CDFs for all prefix and suffix sequences of \mathbf{y} for each feature j . This process is computationally intensive: specifically, constructing the empirical CDFs for the prefix sequences of a feature j necessitates sequentially inserting a new element y_{s+1} into the current sorted version of the list $\mathbf{y}^{(s)}$, with a time complexity of $\mathcal{O}(s)$. Consequently, the basic construction of a distributional regression tree based on the CRPS loss results in a node split with a time complexity of $\mathcal{O}(dn \log(n) \sum_{i=1}^n s) = \mathcal{O}(dn^3 \log n)$, which is not feasible for practical use.

To efficiently train a tree using the CRPS loss, reducing computations is key. Due to the sequential structure of the computation of entropies associated to prefix (resp. suffix) sequences to perform a node split, one can investigate the possibility to rely on iterative schemes to reduce the computational burden of the algorithm. Theorem 1 presents an iterative formula allowing to compute the entropies associated to all prefix sequences for a given feature j . Note that a similar formula is directly obtained from Theorem 1 for suffix sequences by flipping the sign of each entry of the feature vectors $\{\mathbf{x}_i\}_{i=1}^n$. In what follows, we denote by $h_{\text{mirror}}^{(s)}$ the counterpart of the entropies $h^{(s)}$ from Theorem 1 computed under this sign-flipped transformation of the input features.

Theorem 1. *Let us consider a leaf with data $\{(\mathbf{x}_i, y_i)\}_{i=1}^n$ and a given feature j . Assume without loss of generality that $x_{1,j} \leq \dots \leq x_{n,j}$ and let us denote by $\mathbf{y}^{(s)}$ the prefix sequence (y_1, \dots, y_s) of size s and \hat{F}_s the empirical CDF of $\mathbf{y}^{(s)}$. Then, the empirical entropies*

$$H_{\text{CRPS}}(\mathbf{y}^{(s)}) := \frac{1}{s} \sum_{i=1}^s \text{CRPS}(\hat{F}_s, y_i),$$

for all $s \in [n]$ can be computed using an iterative scheme. Indeed, we have

$$H_{\text{CRPS}}(\mathbf{y}^{(s+1)}) = \frac{1}{(s+1)^3} \left(s^3 H_{\text{CRPS}}(\mathbf{y}^{(s)}) + h^{(s+1)} \right),$$

with $h^{(0)} = 0$ and for any $s \geq 1$,

$$h^{(s)} = h^{(s-1)} + (s-1)[2r_s - s]y_{(r_s)}^{(s)} + 2W^{(s)} - 2S^{(s)} - 2(s-1)S_{r_s}^{(s)},$$

and where for any $r \in [s]$,

$$S_r^{(s)} := \sum_{i=1}^r y_{(i)}^{(s)}, \quad W^{(s)} := \sum_{i=1}^s iy_{(i)}^{(s)} \quad \text{and} \quad S^{(s)} := S_s^{(s)},$$

and, for any $s \in [n-1]$, r_{s+1} is the insertion rank of y_{s+1} within the non-decreasing sorted version of the list $\mathbf{y}^{(s)}$.

Theorem 1 shows that training a distributional regression tree using the CRPS loss is achievable if the insertion ranks $(r_s)_{s \in [n]}$ and cumulative sums $S_{r_s}^{(s)}$, $S^{(s)}$, and $W^{(s)}$ can be computed efficiently. To this end, we introduce the *CRPS-Optimal Split* algorithm, which leverages tailored data structures to compute the entropy of all candidate splits for any feature j in $\mathcal{O}(n \log n)$ time. The procedure is presented in Algorithm 1 and described in detail in the remainder of this section. To efficiently compute the ranks r_s , the algorithm uses a Weight-balanced tree. This is a type of self-balancing binary search tree that keeps its shape roughly balanced as elements are inserted or removed. Because of this balance, operations like insertion, deletion, and searching can all be done in $\mathcal{O}(\log n)$ time.

In our case, we use the Weight-balanced tree to determine the rank of each element as it is inserted — that is, how many elements in the current set are smaller than the new one. You can think of it as inserting each value into a dynamically maintained sorted list and instantly knowing its sorted position (its rank), without needing to sort the whole list. This rank computation is also performed in $\mathcal{O}(\log n)$ time thanks to the structure of the tree.

Once we have the ranks $(r_s)_s$, we use a Fenwick tree (also known as a binary indexed tree) to compute the cumulative sums $S_{r_s}^{(s)}$. A Fenwick tree is a clever data structure that allows us to efficiently update values and calculate prefix sums — that is, the sum of values up to a certain index. Unlike a regular array, which would need up to n steps to compute a prefix sum, a Fenwick tree can do it in just $\mathcal{O}(\log n)$ time. It works by storing partial sums in a compact binary format, allowing both updates and queries to be fast. An illustration of how the Fenwick Tree works is shown in Figure 1.

CRPS-Based tree training: Detailed procedure. For a given feature j , the process begins by sorting the list of feature entries $\{x_{i,j}\}_{i=1}^n$, which requires $\mathcal{O}(n \log n)$ time. Once sorted, the insertion ranks $(r_s)_{s \in [n]}$ can be pre-computed using a weight-balanced tree [NR73]. Weight-balanced trees offer logarithmic performance similar to that of red-black and AVL trees but also provide the advantage of indexing elements in logarithmic time. Lemma 1 shows that these ranks can be pre-computed in $\mathcal{O}(n \log n)$ time.

Lemma 1. [MS04, Chapter 10] *A weight-balanced tree with data $\mathbf{y}^{(s)}$ allows inserting a new value y_{s+1} and determining its position in the sorted version of the list $\mathbf{y}^{(s)}$ such that the resulting list remains in non-decreasing order, all in $\mathcal{O}(\log s)$ time.*

Once the ranks $(r_s)_{s \in [n]}$ are computed, we need to obtain the entropies $H_{\text{CRPS}}(\mathbf{y}^{(s)})$ for any prefix sequence $\mathbf{y}^{(s)}$ using the iterative scheme presented in Theorem 1. For this, it is sufficient to query efficiently the sums $S_{r_s}^{(s)}$, $S^{(s)}$ and $W^{(s)}$. Tracking $S^{(s)} = \sum_{i=1}^s y_i$ across iterations is straightforward, as it simply involves adding the new element y_s to $S^{(s-1)}$ at each step s . Moreover, we observe that

$$W^{(s+1)} = W^{(s)} + r_{s+1}y_{s+1} + \sum_{i=r_{s+1}}^s y_{(i)}^{(s)} = W^{(s)} + (1 + r_{s+1})y_{s+1} + S^{(s)} - S_{r_{s+1}}^{(s+1)},$$

where we used that $\sum_{i=r_{s+1}}^s y_{(i)}^{(s)} = \sum_{i=r_{s+1}}^{s+1} y_{(i)}^{(s+1)} - y_{r_{s+1}}^{(s+1)} = S_{r_{s+1}}^{(s+1)} - y_{s+1}$. Thus, maintaining $W^{(s)}$ comes at no additional cost if partial sums of the form $S_{r_s}^{(s)}$ can be queried efficiently. This highlights

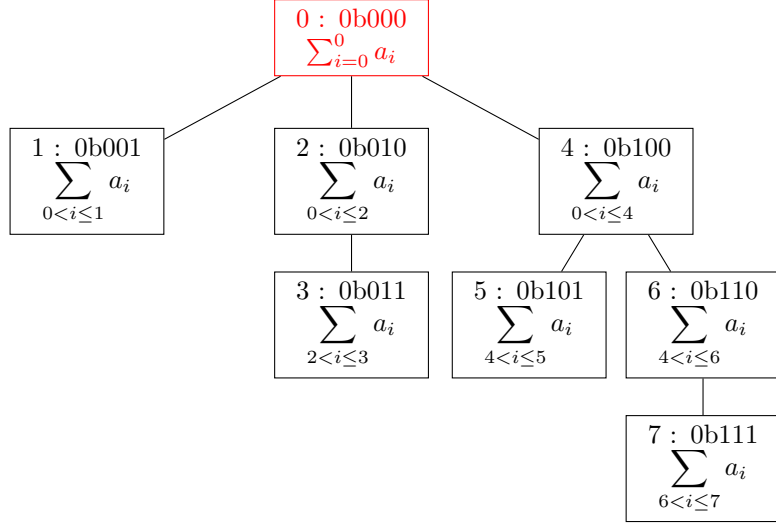


Figure 1: Fenwick tree for a list $(a_i)_{i \in \{1, \dots, 7\}}$ of length 7. By convention, $a_0 = 0$. The nodes of the tree are indexed by the natural integers. 0 is at the root and the children of the root correspond to all integers of the form 2^p with $p \in \mathbb{N}$. More generally, nodes at depth k are the sum of k integers of the form 2^p , i.e., they have k non-zero bits in their binary expansion. The parent of node i has the same binary expansion except that the lowest non-zero bit of i is set to 0 in its parent. If $A_j = \sum_{i=0}^j a_i$, then the partial sum stored at node i is $A_i - A_{\text{pa}(i)}$, where $\text{pa}(i)$ is the parent of i .

that efficiently tracking these sums is the key to designing an algorithm that constructs regression trees for the CRPS loss. Denoting by σ a permutation sorting the list \mathbf{y} in non decreasing order and having in mind that $y_s = y_{(r_s)}^{(s)}$, the crucial observation is:

$$S_{r_s}^{(s)} = \underbrace{\sum_{i=1}^{r_s} y_{(i)}^{(s)}}_{r_s \text{ smallest elements of } \mathbf{y}^{(s)}} = \underbrace{\sum_{i=1}^s 1_{\sigma^{-1}(i) \leq \sigma^{-1}(s)} y_i}_{\text{Elements of } \mathbf{y}^{(s)} \text{ smaller than } y_s} = \underbrace{\sum_{j=1}^{\sigma^{-1}(s)} 1_{\sigma(j) \leq s} y_{\sigma(j)}}_{\text{Elements of } \mathbf{y} \text{ smaller than } y_s \text{ with index } \leq s}. \quad (5)$$

Building on Eq.(5), we rely on a customized Fenwick tree to efficiently track the sums $S_{r_s}^{(s)}$. A Fenwick tree, as shown in Figure 1, is a binary-indexed data structure that efficiently supports prefix sum and insertion in logarithmic time. In Definition 1, we introduce the tailored Fenwick tree \mathcal{F} , which serves as the cornerstone of our algorithm, enabling efficient node splits.

Definition 1. Let us denote by σ a permutation sorting the list \mathbf{y} in non decreasing order (i.e. $y_{\sigma(1)} \leq \dots \leq y_{\sigma(n)}$). We define by \mathcal{F} a Fenwick tree of size n initialized with n zero values such that at any iteration $s \geq 1$, we add the element y_s at the position $\sigma^{-1}(s)$ in the list represented by the Fenwick tree \mathcal{F} .

By construction at any iteration s , \mathcal{F} is a Fenwick tree for the list $(1_{\sigma(i) \leq s} y_{\sigma(i)})_{i \in [n]}$. In Lemma 2, we demonstrate that \mathcal{F} enables tracking the cumulative sums of the form $S_{r_s}^{(s)}$ and $S^{(s)}$ which, as a by product, allows for monitoring $W^{(s)}$ throughout the iterative process. The proof of Lemma 2 is provided in Section C.2.

Lemma 2. At iteration s , the structure of the Fenwick tree \mathcal{F} makes it possible to:

- calculate $S_{r_s}^{(s)}$ and $S^{(s)}$ in $\mathcal{O}(\log n)$ time,
- insert a new value in $\mathcal{O}(\log n)$ time,
- compute $W^{(s)}$ from $W^{(s-1)}$ in $\mathcal{O}(\log n)$ time.

Algorithm 1 CRPS-Optimal Split: Optimal CRPS Node Split for feature j

- 1: **Input:** Feature values $\mathbf{x}_{:,j}$ and target vector $\mathbf{y} = (y_1, \dots, y_n)$, sorted such that $x_{1,j} \leq \dots \leq x_{n,j}$
- 2: Let σ be the permutation sorting \mathbf{y} in non-decreasing order: $y_{\sigma(1)} \leq \dots \leq y_{\sigma(n)}$
- 3: Initialize: $W^{(0)} \leftarrow 0$, $h^{(0)} \leftarrow 0$
- 4: **For** $s = 1$ to n **do**:

Computation	Operation & Data Structure	Time Complexity
Compute rank r_s	Query rank via inserting y_s in a Weight-balanced tree	$\mathcal{O}(\log n)$
Compute partial sum $S_{r_s}^{(s)} = \sum_{i=1}^{r_s} y_{(i)}^{(s)}$	Insert the value y_s and query the prefix sum from 1 to $\sigma^{-1}(s)$ in the Fenwick Tree	$\mathcal{O}(\log n)$
Update weighted sum $W^{(s)}$	Incremental update from $W^{(s-1)}$ and $S_{r_s}^{(s)}$	$\mathcal{O}(1)$
Update entropy $h^{(s)}$	Closed-form update using $W^{(s)}$, $h^{(s-1)}$, and $S_{r_s}^{(s)}$	$\mathcal{O}(1)$

- 5: Repeat the above loop with \mathbf{y} in reverse order to obtain $h_{\text{mirror}}^{(s)}$
- 6: **Output:** Optimal split index $s^*(j)$ and the corresponding entropy

$$s^*(j) = \arg \min_s \left(s \cdot h^{(s)} + (n - s) \cdot h_{\text{mirror}}^{(s)} \right)$$

In Section B.2, we present in details our algorithm to perform a node split to grow a CRPS-RT. Overall, the computational time required to perform a node split scales as $\mathcal{O}(dn \log n)$ where n is the number of data points in the node and d is the number of features. The time complexity of the two algorithms presented in this paper are given in Table 1.

Algorithm	Multiple Quantiles Regression Tree	CRPS Regression Tree
Time complexity	$\mathcal{O}(Md n \log n)$	$\mathcal{O}(dn \log n)$

Table 1: Worst case time complexity for a specific node split for the different regression trees.

2.4 Unbiased estimate of the entropies using leave-one-out

To train PQRTs, PMQRTs or CRPS-RTs, we proposed in the previous sections to rely on the standard CART algorithm [BFSO84] which leads to biased estimates of entropies. This bias arises because the same data is used both to estimate parameters (such as empirical quantiles or cumulative distribution functions) and to compute the entropies. By doing so, the empirical entropies computed at any step of the training procedure is a biased estimate of the target entropy. A naive solution to mitigate this issue involves splitting the data into two disjoint sets—one for parameter estimation and the other for entropy evaluation. However, such a data-splitting approach is statistically suboptimal since only part of the data is used at each step. To overcome this limitation, we adopt a leave-one-out (LOO) approach which provides unbiased entropy estimates. The LOO method estimates a quantity by systematically removing one data point at a time, computing the desired statistic on the remaining data, and averaging the results over all possible leave-one-out subsets. The pitfall is that the naive implementation of this method is computationally heavy. Fortunately, we show that this LOO estimate of the entropy can be obtained at no additional cost for both the CRPS loss and the pinball loss. Proposition 1 establishes that the LOO estimate of empirical entropy for the CRPS loss, $H_{\text{CRPS}}^{\text{LOO}}(\mathbf{y})$, is simply a scaled version of $H_{\text{CRPS}}(\mathbf{y})$.

Proposition 1. Let H_{CRPS} denote the entropy of \mathbf{y} for the pinball loss ℓ_τ and $H_{\text{CRPS}}^{\text{LOO}}$ its LOO version, defined as:

$$H_{\text{CRPS}}(\mathbf{y}) = \frac{1}{n} \sum_{i=1}^n \text{CRPS}(\widehat{F}_n, y_i), \quad H_{\text{CRPS}}^{\text{LOO}}(\mathbf{y}) = \frac{1}{n} \sum_{i=1}^n \text{CRPS}(\widehat{F}_n^{-i}, y_i),$$

where \widehat{F}_n and \widehat{F}_n^{-i} represent the empirical CDF of \mathbf{y} and $\mathbf{y}^{-i} = (y_1, \dots, y_{i-1}, y_{i+1}, \dots, y_n)$, respectively. We have

$$H_{\text{CRPS}}^{\text{LOO}}(\mathbf{y}) = \frac{n^2}{(n-1)^2} H_{\text{CRPS}}(\mathbf{y}).$$

Proposition 2 shows that the LOO estimate of empirical entropy for the pinball loss, $H_{\ell_\tau}^{\text{LOO}}(\mathbf{y})$, can be derived from $H_{\ell_\tau}(\mathbf{y})$ by adding a debiasing term that depends on $y_{(r^*-1)}$, $y_{(r^*)}$, and $y_{(r^*+1)}$, where $r^* := \lceil n\tau \rceil$. Since these values can be retrieved in constant time using the min-max heap structures described in Section 2.2, a node split, whether using LOO or not, is still performed in $\mathcal{O}(dMn \log n)$ time when considering a sum of M pinball losses. The proofs of Propositions 2 and 1 are presented in Section D.

Proposition 2. Let H_{ℓ_τ} denote the entropy of \mathbf{y} for the pinball loss ℓ_τ and $H_{\ell_\tau}^{\text{LOO}}$ its LOO version, defined as:

$$H_{\ell_\tau}(\mathbf{y}) = \frac{1}{n} \sum_{i=1}^n \ell_\tau(y_i, \hat{q}_\tau), \quad H_{\ell_\tau}^{\text{LOO}}(\mathbf{y}) = \frac{1}{n} \sum_{i=1}^n \ell_\tau(y_i, \hat{q}_\tau^{-i}),$$

where \hat{q}_τ and \hat{q}_τ^{-i} represent the empirical quantiles of order τ computed over \mathbf{y} and $\mathbf{y}^{-i} = (y_1, \dots, y_{i-1}, y_{i+1}, \dots, y_n)$, respectively. Setting $r^- := \lceil \tau(n-1) \rceil$ and $r^* := \lceil n\tau \rceil$, we have

$$H_{\ell_\tau}^{\text{LOO}}(\mathbf{y}) = \begin{cases} H_{\ell_\tau}(\mathbf{y}) + (1-\tau)r^*(y_{(r^*+1)} - y_{(r^*)}) & \text{if } r^* = r^- \\ H_{\ell_\tau}(\mathbf{y}) + \tau(n-r^*+1)(y_{(r^*)} - y_{(r^*-1)}) & \text{if } r^* = r^- + 1. \end{cases}$$

2.5 Algorithms in practice

In this section we provide concrete examples to illustrate how our algorithms to learn PMQRT or CRPS-RT update the data structures (respectively min-max heaps and Fenwick trees) along the iterations. Figure 2 gives a concrete example on the way the min-max heaps are updated at a given iteration to perform a node split in a PMQRT. We consider as loss function the sum of two pinball losses with quantile levels respectively 0.3 and 0.7. We assume that we need to identify the best split for a given feature j for which $x_{1,j} \leq \dots \leq x_{7,j}$ with corresponding observations $\mathbf{y} = [0, 1, 2, 3, -1, -2, -3]$. In Figure 2, we illustrate the evolution of the three min-max heaps \mathcal{H}_1 , \mathcal{H}_2 and \mathcal{H}_3 from iteration 5 to 6 to compute the entropies associated to the prefix sequences $\mathbf{y}^{(6)}$. Next to each heap, the blue value represents the sum of all elements within the corresponding heap.

Figure 3 illustrates the updates of the Fenwick tree to perform a node split in a CRPS-RT. Similarly to Figure 2, we assume that we need to identify the best split for a given feature j for which $x_{1,j} \leq \dots \leq x_{6,j}$ with corresponding observations $\mathbf{y} = [2, 1, 3, -1, -3, -2]$.

3 Experiments

3.1 CDF estimation improvement with an unbiased CRPS risk estimate

To demonstrate the importance of using LOO for calculating information gain, we consider a simple example where the covariate X is uniformly sampled from the interval $(0, 10)$, and

$$Y \mid X \sim \text{Gamma}(\text{shape} = \sqrt{X}, \text{scale} = \min\{\max\{X, 1\}, 6\}) \quad (\text{Gamma})$$

Figure 4 shows the estimated conditional CDFs using a forest of 100 CRPS-RTs, comparing the results with and without LOO used for entropy calculation. On this example, applying LOO produces a significantly better estimate of the conditional CDFs. We perform a similar experiment for PMQRF, demonstrating a significant improvement in quantile estimates achieved through the use of LOO. The results of these simulations are presented in Section D.

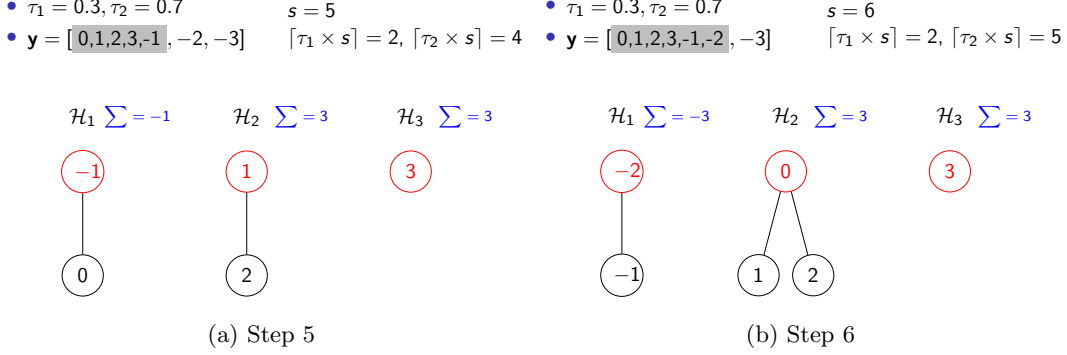


Figure 2: Illustration of an update of the min-max heaps at a specific iteration of the algorithm to perform a node split in a PMQRT. We consider the sum of pinball losses with quantile levels 0.3 and 0.7. At step 6, we need to insert $y_6 = -2$ in the min-max heaps. \mathcal{H}_1 must contain $\lceil \tau_1 \times 6 \rceil = 2$ elements and it already contains two elements. Since -2 is smaller than the current maximum element of \mathcal{H}_1 (namely 0), we pop out 0 and insert -2 in \mathcal{H}_1 . Now, we need to insert 0 in one of the remaining heaps $\mathcal{H}_2, \mathcal{H}_3$. \mathcal{H}_2 must contain $\lceil \tau_2 \times 6 \rceil - \lceil \tau_1 \times 6 \rceil = 5 - 2 = 3$ elements, and it currently contains 2 elements. Since 0 is smaller than the current maximum value in \mathcal{H}_2 (namely 2), we insert 0 in \mathcal{H}_2 and the update is completed.

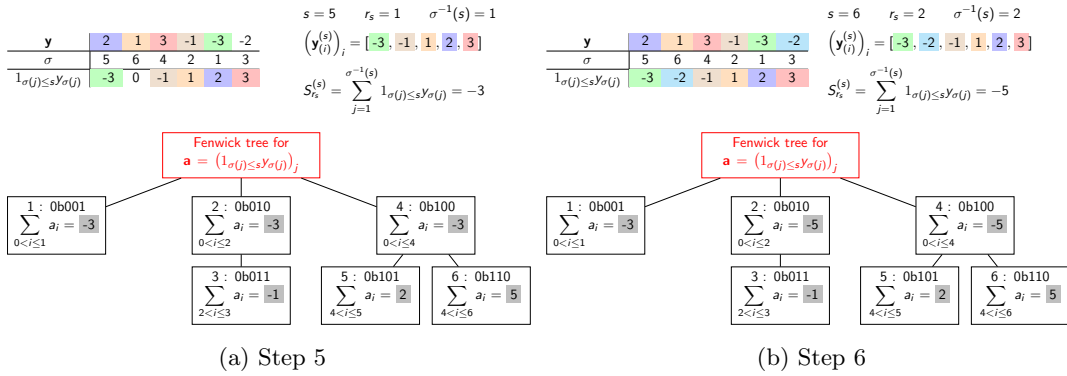


Figure 3: Illustration of an update of the Fenwick tree at a specific iteration of the algorithm to perform a node split in a CRPS-RT. We first insert $y_s = -2$ in the Fenwick tree at the position $\sigma^{-1}(s)$, with $s = 6$. Then, we know that querying the prefix sum up to index $\sigma^{-1}(s)$ will give us the partial sum $S_{r_s}^{(s)}$, needed to update the entropy.

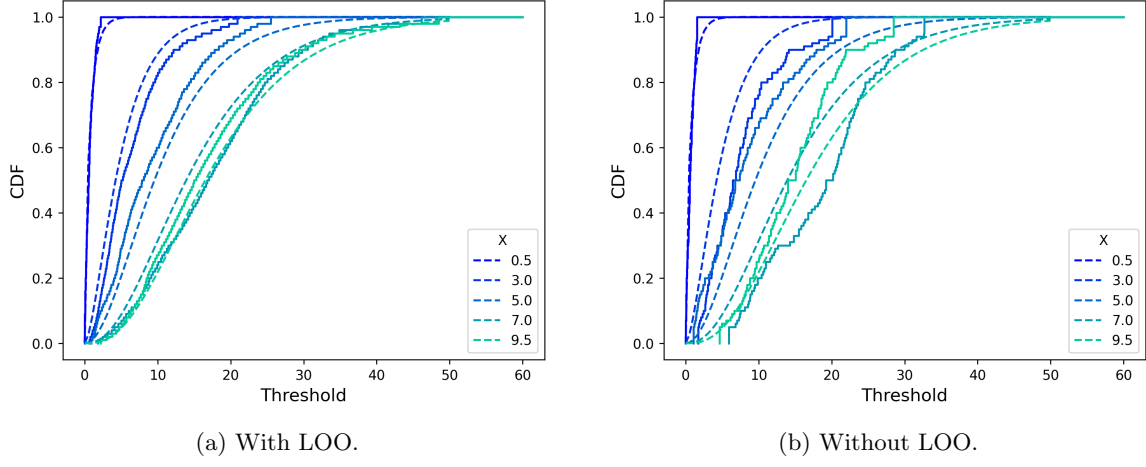


Figure 4: Estimation of the conditional CDF of y given x with CRPS-RF on a sample of size $n = 600$ simulated from the distribution in Eq.([Gamma](#)). The true conditional CDFs (smooth dashed lines) are compared to the estimates obtained from CRPS-RF (solid line step functions).

3.2 Computational time

In this section, we conduct experiments to assess the scalability of our method to learn regression trees minimizing the CRPS loss. First, we consider random vectors (y_1, \dots, y_n) with i.i.d. entries sampled from a white noise Gaussian distribution and we compute the empirical entropy $H_{\text{CRPS}}(\mathbf{y}^{(s)})$ associated to all prefix sequences $\mathbf{y}^{(s)} = (y_1, \dots, y_s)$ for all $s \in [n]$, namely

$$H_{\text{CRPS}}(\mathbf{y}^{(s)}) := \frac{1}{s} \sum_{i=1}^s \text{CRPS}(\widehat{F}^{(s)}, y_i),$$

where $\widehat{F}^{(s)}$ is the empirical CDF of sequence $\mathbf{y}^{(s)}$. We compare with a method computing all CRPS independently using available Python packages. Figure 5 demonstrates the computational time required for a node split during the training of a regression tree that minimizes the CRPS loss. When naively computing all CRPS values, the time complexity scales empirically as $O(n^{2.55})$. In contrast, the method proposed in this paper has a computational time complexity that scales as $O(n \log n)$, as theoretically demonstrated.

3.3 Comparing CRPS-RF and PMQRF with QRF

In this section, we describe the numerical experiments conducted to evaluate the performance of our models. We selected five datasets from the UCI Machine Learning Repository to cover a variety of real-world applications. The total number of samples n , the number of features d , and the URL for each dataset are provided in Table 2. For each dataset, we randomly sampled 1,000 data points without

Dataset	n	d	URL
Abalone	4177	8	abalone
Turbine	36733	12	gas+turbine+co+and+nox+emission+data+set
Cycle	9568	4	combined+cycle+power+plant
WineRed	4898	11	wine-quality/winequality-red.csv
WineWhite	1599	11	wine-quality/winequality-white.csv

Table 2: Meta-data for the datasets. n refers to the total number of data-points from which we create 300 versions by independently drawing 1000 data points randomly (as described in the beginning of Section 3.3). d refers to the feature dimension.

replacement to generate the training sets, while the remaining data points were used as the test set to compute the prediction error. We consider forests of PMQRTs or CRPS-RTs with 50 trees. Trees

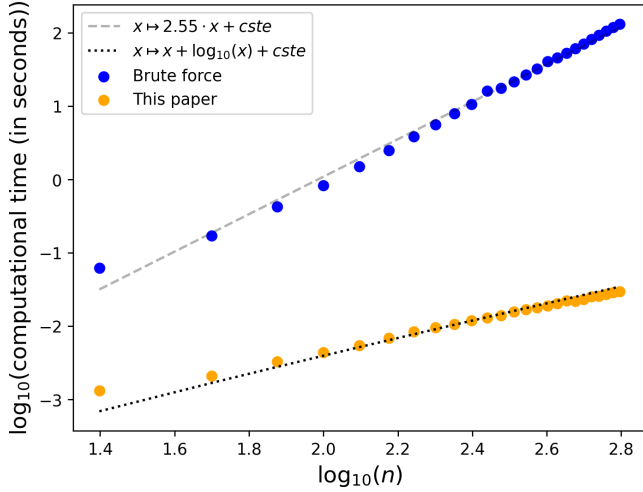


Figure 5: Time to compute the CRPS of the prefix sequences $\mathbf{y}^{(s)} = (y_1, \dots, y_s)$ for all $s \in [n]$ where y_1, \dots, y_n are sampled independently from a standard normal distribution. For the brute force approach, we compute the CRPS using the *properscorer* Python package.

in the forests are trained by sampling uniformly at random without replacement 60% of the training data. This procedure was repeated for 300 different training sets, each generated by sampling the data points randomly. We computed the mean and standard deviation of the CRPS on the test set across these 300 experiments, which are reported in Table 3. For each method, the CRPS was computed on the test set by querying quantiles with level $\mathcal{Q}_{0.02} := \{0.02 \times k, \ k \in [50]\}$ and building the corresponding CDF.

To train the PMQRTs, we used predefined lists of quantile levels ranging from 0.1 to 0.9 with either a step size of 0.1 (referred to as PMQRF step 0.1) or a step size of 0.05 (referred to as PMQRF step 0.05). To benchmark our model, we compared its performance with that of the Quantile Regression Forest (QRF) method.

An important aspect of the tree-based methods such as QRF, PMQRT, and CRPS-RF is that they rely on trees learning a single partition of the feature space for all quantile levels. This common partitioning has certain advantages, such as facilitating group conformal prediction (see Section 3.4 for more details) and ensuring that the estimated quantiles are non-crossing. However, for some data distributions, the use of a single partition for all quantiles can lead to suboptimal results. To assess the cost of using a common partition for all quantile levels, we compared the aforementioned methods with a quantile regression model from the Scikit-learn library (SKLearn), where an independent model is trained for each quantile level. This allows for more flexible partitioning of the feature space, though it comes at the cost of losing the benefits of a shared partition. We provide in Table 4 the percentage of crossing quantiles when training and evaluating the quantile regression method from Scikit-learn using either the list of quantile levels $\mathcal{Q}_{0.05}$ or $\mathcal{Q}_{0.01} := \{0.01, 0.02, \dots, 0.99\}$. More precisely, the percentage of crossing quantiles reported is the average over 100 simulations of the following quantity:

$$\frac{1}{\frac{1}{step} - 1} \sum_{m=1}^{\frac{1}{step}-1} \frac{1}{|\mathcal{D}_{\text{test}}|} \sum_{i \in \mathcal{D}_{\text{test}}} \mathbf{1}\{\hat{q}_{\tau_m}(x_i) > \hat{q}_{\tau_{m+1}}(x_i)\}, \quad (6)$$

for $step = 0.05$ (respectively 0.01) when considering $\mathcal{Q}_{0.05}$ (respectively $\mathcal{Q}_{0.01}$). In Eq. (6), $\mathcal{D}_{\text{test}}$ represents the test set and $\hat{q}_\tau(x_i)$ is the predicted quantile for input x_i at quantile level τ .

Table 3 highlights SKLearn as the worst performer, with consistently the largest CRPS on the test set across all datasets, except for the Turbine dataset, where SKLearn notably outperforms the other methods. These results suggest that training a method capable of learning multiple quantiles (or even the entire conditional distribution) can lead to improved model accuracy. However, for certain data distributions, it may be beneficial to partition the feature space differently for different quantile levels. In the case of the Turbine dataset, using a single partition for learning multiple conditional quantiles simultaneously appears to hinder performance. To address this, one potential solution is to train two

separate PMQRTs: one targeting quantiles below 50%, and the other targeting those above 50%.

PMQRFs generally deliver better results than QRFs, particularly when trained with a larger number of quantiles. As the number of quantile levels increases, the performance of PMQRFs becomes closer to that of CRPS-RF, which aligns with the theoretical convergence of the WIS to the CRPS. However, CRPS-RF consistently outperforms all tree-based methods across the datasets. This demonstrates the advantage of using a loss function that directly considers the entire conditional distribution, rather than focusing on point estimates or specific quantiles.

Method	Abalone	Turbine	Cycle	WineRed	WineWhite
QRF	1.92 (0.11)	1.55 (0.17)	4.15 (0.17)	0.57 (0.06)	0.68 (0.07)
PMQRF (step 0.1)	1.88 (0.09)	1.53 (0.16)	4.20 (0.16)	0.56 (0.06)	0.65 (0.07)
PMQRF (step 0.05)	1.87 (0.07)	1.50 (0.15)	4.12 (0.15)	0.55 (0.05)	0.63 (0.06)
CRPS-RF	1.81 (0.06)	1.43 (0.14)	4.05 (0.14)	0.51 (0.05)	0.60 (0.06)
SKLearn	1.95 (0.12)	0.60 (0.10)	4.40 (0.12)	0.62 (0.06)	0.72 (0.05)

Table 3: For each method and dataset, the first value represents the mean of the CRPS on the test set, while the second value in parentheses indicates the standard deviation of the error across the 300 simulations.

List of quantile levels (for training and prediction)	Abalone	Turbine	Cycle	WineRed	WineWhite
$Q_{0.05}$	1.6%	2.4%	0.2%	8.5%	2.8%
$Q_{0.01}$	9.6%	12.6%	5.0%	17.3%	14.4%

Table 4: Percentage of crossing quantiles using the quantile regression method from the Scikit-learn Python library (averaging over 300 simulations).

3.4 Adaptive group conformal prediction with CRPS random trees

In this section, we show how CRPS-RTs can be used to achieve group conformal prediction. Inspired by the simulated dataset from [SC20], we consider data $\{(\mathbf{x}_i, y_i)\}_{i=1}^n$ where

$$\forall i \in [n], \quad y_i = f(\mathbf{x}_i^\top \beta) + \epsilon_i \sqrt{1 + (\mathbf{x}_i^\top \beta)^2}, \quad (7)$$

with $\beta = [1, 1] \in \mathbb{R}^2$, $\mathbf{x}_i \sim \text{Unif}([0, 1]^2)$ are independent vectors, and $(\epsilon_i)_{i \in [n]}$ are independent standard normal random variables.

We train a single CRPS-RT with a training set of size $n = 2000$. We define four regions corresponding to the partition of the feature space obtained from the CRPS-RT at depth 2. We then evaluated different conformalized predictive inference methods, based on CRPS-RF or QRF with 50 trees, with both marginal and group-based conformalization considering the four previously defined groups. Our goal is to assess how well these methods achieve the desired coverage while maintaining narrow prediction intervals across the different regions.

We use the split conformal framework to conformalize the different methods. To do so, we consider a calibration set with 1000 data points and a test set of 5000 points. We conformalize the CRPS-RF method by considering the family of nested sets presented in [CWZ21], namely of the form

$$[\hat{q}_t(\mathbf{x}), \hat{q}_{1-t}(\mathbf{x})],$$

where $\hat{q}_t(\mathbf{x})$ denotes the empirical quantile of level t obtained from our CRPS-RT by dropping the feature vector $\mathbf{x} \in [0, 1]^2$ from the root in the CRPS-RT and by taking the empirical quantile of

level t from the data points in the leaf where we end up. We compare our method with a similar split conformal method obtained by training QRF and conformalizing using the CQR method from [RPC19]. In both case, we target a marginal coverage of $90\% = 1 - \alpha$.

Figure 6 illustrates the impact of different conformalization strategies on coverage and mean prediction interval width across the four regions identified by the CRPS-RT partitioning. Notably, the QRF-CQR method without group conformalization results in highly unbalanced coverage, failing to maintain the desired coverage level uniformly across the regions. This suggests that standard marginal conformalization struggles to adapt to the heterogeneity present in the learned feature space partition. In contrast, the CRPS-RF method with a distributional nested set and marginal calibration naturally provides better balance in coverage across the four regions. This improved calibration highlights the advantage of leveraging CRPS-based probabilistic forests for predictive inference.

Among all the methods considered, the group-conformalized CRPS-RF approach emerges as the most effective. It not only achieves the target coverage across all four regions but also maintains the narrowest marginal mean prediction interval width. This demonstrates that incorporating group-based conformalization within CRPS-RF leads to both improved calibration and sharper predictive intervals, making it the most reliable approach in this setting.

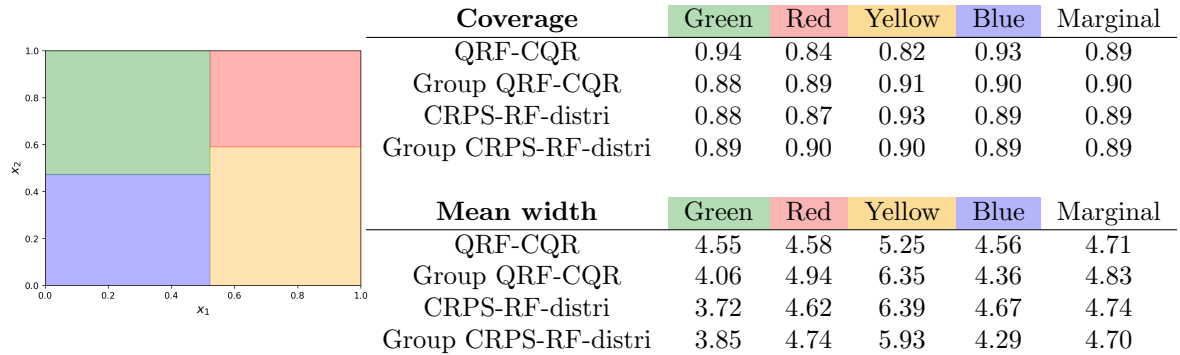


Figure 6: We train a single CRPS-RT and identify four distinct regions in the feature space, based on the learned partition induced by the CRPS-RT at depth 2. We evaluate the performance of conformalized predictive inference methods, including CRPS-RF (with both marginal and group-based conformalization) and QRF-CQR. For each method, we report the coverage and mean prediction interval width across the four regions.

4 Conclusion

We introduced two new algorithms for learning regression trees: one using the sum of pinball losses to estimate multiple quantiles with a single model, and the second based on the CRPS. These regression trees can serve as the foundation for introducing novel conformal prediction methods, in particular by enhancing the quantile out-of-bag conformal ensemble method introduced by [GKR22].

A List of notations

$\mathbf{y}^{(s)}$	Prefix sequence (y_1, \dots, y_s) of the list (y_1, \dots, y_n)
$\mathbf{y}_{(i)}^{(s)}$	i -th larger element of the list $\mathbf{y}^{(s)}$
r_s	The position to insert the element y_s into the list $(y_{(1)}^{(s-1)}, \dots, y_{(s-1)}^{(s-1)})$ in order to maintain its non decreasing order
$S^{(s)}$	$\sum_{i=1}^s y_{(i)}^{(s)} = \sum_{i=1}^s y_i$
$S_r^{(s)}$	$\sum_{i=1}^r y_{(i)}^{(s)}$
$W^{(s)}$	$\sum_{i=1}^s iy_{(i)}^{(s)}$
σ	Permutation sorting the list \mathbf{y} in increasing order, i.e. $y_{\sigma(1)} \leq \dots \leq y_{\sigma(n)}$
$\cdot.get(a, b)$	Operator acting on a Fenwick tree that outputs the cumulative sum of the elements from position a to position b (both included) in the corresponding tree.

B Algorithms pseudo-codes for PMQRTs and CRPS-RTs

B.1 Computations of the entropies for all splits for multiple quantiles

We consider M quantile levels: $\tau_1 < \dots < \tau_M$. In this section, we provide the detailed algorithm to train regression trees to minimize the empirical entropy associated with a sum of the pinball losses with quantile levels τ_1, \dots, τ_M . By convention, querying the minimum or the maximum of an empty heap returns a `None` value. Moreover, each min-max heap data structure keeps track of the total sum of the current elements within the heap.

Algorithm 2 describes the procedure to compute the information gain induced by all the possible splits at a given node.

Algorithm 2 PMQRT: Returns the feature index and the threshold value giving the split of the data with the largest information gain.

```

1: Input: Data in a given node of the leaf  $\{(\mathbf{x}_i, y_i)\}_{i=1}^n$ 
2:  $score^*, split^*, feature^* \leftarrow +\infty, None, None$ 
3: for  $j = 1$  to  $d$  do
4:   Let  $x_{i_1, j} \geq \dots \geq x_{i_n, j}$  be the decreasing sorted  $(x_{i,j})_{i \in [n]}$  and set  $\mathbf{y} := (y_{i_1}, \dots, y_{i_n})$ .
5:    $\ell_{\mathcal{E}}^{\downarrow} \leftarrow \text{GetEntropiesPMQRT}(\mathbf{y})$  /* cf. Algorithm 3
6:   Let  $x_{i_1, k} \leq \dots \leq x_{i_n, k}$  be the increasing sorted  $(x_{i,k})_{i \in [n]}$  and set  $\mathbf{y} := (y_{i_1}, \dots, y_{i_n})$ .
7:    $\sigma \leftarrow \text{ArgSort}(\mathbf{y})$ 
8:    $\ell_{\mathcal{E}}^{\uparrow} \leftarrow \text{GetEntropiesPMQRT}(\mathbf{y})$  /* cf. Algorithm 3
9:    $w^*, score \leftarrow \text{ArgMin}(w \times \ell_{\mathcal{E}}^{\uparrow}[w] + (n - w) \times \text{Flip}(\ell_{\mathcal{E}}^{\downarrow})[w], w \in \{0, \dots, n\})$ 
10:  if  $score < score^*$  then
11:     $score^*, split^*, feature^* \leftarrow score, x_{i_{w^*}, j}, j$ 
12:  end if
13: end for
14: Return  $split^*, feature^*$ 

```

Algorithm 3 GetEntropiesPMQRT

Input: List of values in the leaf \mathbf{y}
Initialize empty min-max heaps \mathcal{H}_m for $m \in \{1, \dots, M+1\}$ and insert y_1 in \mathcal{H}_1 .
 $\ell_{\mathcal{E}} \leftarrow [0 \text{ , get_entropy}((\mathcal{H}_m)_{m \in [M+1]}, 1)]$ /* cf. Algorithm 6

for $s = 2$ to n_k **do**

$\tilde{y} \leftarrow y_{i_s}$

for $m = 1$ to M **do**

if $\sum_{\ell=1}^m |\mathcal{H}_\ell| = \lceil \tau_{ms} \rceil + 1$ **then**

if \mathcal{H}_m is not empty and $\tilde{y} \leq \max(\mathcal{H}_m)$ **then**

Remove the maximum $A_{j,k,s,m}$ of \mathcal{H}_m .

Insert \tilde{y} in \mathcal{H}_m .

$\tilde{y} \leftarrow A_{j,k,s,m}$.

end if

else

$\hat{m}, \hat{a}_{j,k,s,m} \leftarrow \text{get_min_heaps_plus}(m+1)$ /* cf. Algorithm 5

if $(\hat{a}_{j,k,s,m} \text{ is } \text{None})$ or $(\tilde{y} \leq \hat{a}_{j,k,s,m})$ **then**

Insert \tilde{y} in \mathcal{H}_m .

if $\hat{a}_{j,k,s,m} \text{ is } \text{None}$ **then**

$\tilde{y} \leftarrow \text{None}$

break

else

Remove the min $\hat{a}_{j,k,s,m}$ of $\mathcal{H}_{\hat{m}}$

$\tilde{y} \leftarrow \hat{a}_{j,k,s,t}$

end if

else

Remove the min $\hat{a}_{j,k,s,m}$ of $\mathcal{H}_{\hat{m}}$

Insert $\hat{a}_{j,k,s,m}$ in \mathcal{H}_t

end if

end if

end for

if \tilde{y} is not None **then**

Insert \tilde{y} in \mathcal{H}_{M+1} .

end if

$\ell_{\mathcal{E}}.\text{append}(\text{get_entropy}((\mathcal{H}_m)_{m \in [M+1]}, s))$ /* cf. Algorithm 6

end for

Algorithm 4 Get max value among heaps below a given index.

procedure GET_MAX_HEAPS_MINUS(idx_heap)

max_val = None

while $(\text{idx_heap} \geq 0)$ and $(\text{max_val} \text{ is } \text{None})$ **do**

max_val $\leftarrow \max(\mathcal{H}_{\text{idx_heap}})$

if max_val is None **then**

idx_heap $\leftarrow \text{idx_heap} - 1$

end if

end while

return idx_heap, max_val

end procedure

Algorithm 5 Get min value among heaps above a given index.

```
procedure GET_MIN_HEAPS_PLUS(idx_heap)
    min_val = None
    while (idx_heap < M + 1) and (min_val is None) do
        min_val ← min( $\mathcal{H}_{idx\_heap}$ )
        if min_val is None then
            idx_heap ← idx_heap + 1
        end if
    end while
    return idx_heap, min_val
end procedure
```

Algorithm 6 Get current entropy from the min-max heaps.

```
procedure GET_ENTROPY( $(\mathcal{H}_m)_{m \in [M+1]}$ , n)
    entropy = 0
    heap2sums ← ( $\mathcal{H}_m.sum()$  for  $m \in [M + 1]$ )
    total_sum ← sum(heap2sums)
    cum_sum ← cumsum(heap2sums)
    for  $m = 1$  to  $M$  do
         $-, max\_heap\_m = get\_max\_heaps\_minus(m)$  /* cf. Algorithm 4
        entropy += max_heap_m . ( $\lceil n\tau_m \rceil / n - \tau_m$ )
        entropy += tot_sum .  $\tau_m / n$ 
        entropy -= cum_sum[m] / n
    end for
    return entropy
end procedure
```

B.2 Computations of the entropies for all splits with the CRPS

Theorem 1 ensures that one can compute the information gain at a given node for the possible split of the data points in that node by:

1. computing the insertion ranks $(r_s)_{s \in [n]}$ before running the iterative scheme. This can be done in time complexity $\mathcal{O}(n \log n)$ using a weight-balanced binary tree.
2. updating along the iterative process a Fenwick tree \mathcal{F} that will allow us at iteration s to query $S_{r_s}^{(s)}, S^{(s)}$ and $W^{(s)}$ in $\mathcal{O}(\log n)$ time.

Algorithm 7 describes the procedure to compute the information gain induced by all the possible splits at a given node.

Algorithm 7 CRPS-RT: Returns the feature index and the threshold value giving the split of the data with the largest information gain.

```

1: Input: Data in a given node of the leaf  $\{(\mathbf{x}_i, y_i)\}_{i=1}^n$ 
2:  $score^*, split^*, feature^* \leftarrow +\infty, None, None$ 
3: for  $j = 1$  to  $d$  do
4:   Let  $x_{i_1,j} \geq \dots \geq x_{i_n,j}$  be the decreasing sorted  $(x_{i,j})_{i \in [n]}$  and set  $\mathbf{y} := (y_{i_1}, \dots, y_{i_n})$ .
5:    $\sigma \leftarrow \text{ArgSort}(\mathbf{y})$ 
6:    $\mathbf{r} \leftarrow \text{GetRanks}(\mathbf{y})$  /* cf. Lemma 1
7:    $\ell_{\mathcal{E}}^{\downarrow} \leftarrow \text{GetEntropiesCRPS}(\mathbf{y}, \sigma, \mathbf{r})$  /* cf. Algorithm 8
8:   Let  $x_{i_1,k} \leq \dots \leq x_{i_n,k}$  be the increasing sorted  $(x_{i,k})_{i \in [n]}$  and set  $\mathbf{y} := (y_{i_1}, \dots, y_{i_n})$ .
9:    $\sigma \leftarrow \text{ArgSort}(\mathbf{y})$ 
10:   $\mathbf{r} \leftarrow \text{GetRanks}(\mathbf{y})$  /* cf. Lemma 1
11:   $\ell_{\mathcal{E}}^{\uparrow} \leftarrow \text{GetEntropiesCRPS}((y_{i_1}, \dots, y_{i_n}), \sigma, \mathbf{r})$  /* cf. Algorithm 8
12:   $w^*, score \leftarrow \text{ArgMin}(w \times \ell_{\mathcal{E}}^{\uparrow}[w] + (n - w) \times \text{Flip}(\ell_{\mathcal{E}}^{\downarrow})[w], w \in \{0, \dots, n\})$ 
13:  if  $score < score^*$  then
14:     $score^*, split^*, feature^* \leftarrow score, x_{i_{w^*},j}, j$ 
15:  end if
16: end for
17: Return  $split^*, feature^*$ 

```

Algorithm 8 GetEntropiesCRPS

```

1: Input: List of values in the leaf  $\mathbf{y}$ , Permutation sorting the list  $\sigma$ , ranks  $\mathbf{r}$ 
2:  $S, W, h \leftarrow 0$  Initialization
3:  $\mathcal{F} \leftarrow$  Empty Fenwick Trees of size  $n$ 
4:  $\ell_{\mathcal{E}} \leftarrow [0]$ 
5: for  $s = 1$  to  $n$  do
6:    $W \leftarrow W + r_s y_s + S - \mathcal{F}.\text{get}(1, \sigma^{-1}(s))$  Compute entropy
7:    $S \leftarrow S + y_s$ 
8:    $h \leftarrow h + (s - 1)(2r_s - 3 - (s - 1))y_s + 2W - 2S - 2(s - 1)\mathcal{F}.\text{get}(1, \sigma^{-1}(s))$ 
9:    $\ell_{\mathcal{E}}.\text{append}(h/s^3)$  /* or if using LOO and  $s \neq 1$  :  $h/[s(s - 1)^2]$ 
10:   $\mathcal{F}.\text{add}(\sigma^{-1}(s), y_s)$  /* cf. Algorithm 9 Update tree
11: end for
12: Return  $\ell_{\mathcal{E}}$ 

```

Algorithm 9 Add for Fenwick Tree.

Input: position idx , value z , length n
while $idx \leq n$ **do**
 $self.tree[idx - 1] \leftarrow self.tree[idx - 1] + z$
 $idx = idx + (idx \&^ 1 - idx)$
end while

/* ¹The operator $\&$ compares the binary representations of the two numbers, bit by bit, returning a new integer where each bit is set to 1 only if both bits in the same position are 1.

C Proofs

C.1 Proof of Theorem 1

The CRPS is defined by

$$\text{CRPS}(F, y) = \int_{-\infty}^{+\infty} (F(s) - \mathbb{1}_{s \geq y})^2 ds.$$

The associated entropy is

$$\min_F \mathbb{E}[\text{CRPS}(F, Y)].$$

Considering its empirical counterpart, the minimizer is the empirical CDF.

$$\hat{F} : s \mapsto \frac{1}{n} \sum_{i=1}^n \mathbb{1}_{s \geq y_i}.$$

We deduce that the empirical entropy is given by

$$\begin{aligned} & \frac{1}{n} \sum_{i=1}^n \text{CRPS}(\hat{F}, y_i) \\ &= \frac{1}{n} \sum_{i=1}^n \int_{-\infty}^{+\infty} (\hat{F}(s) - \mathbb{1}_{s \geq y_i})^2 ds \\ &= \frac{1}{n} \sum_{i=1}^n \int_{-\infty}^{+\infty} \left(\frac{1}{n} \sum_{j=1}^n \mathbb{1}_{s \geq y_j} - \mathbb{1}_{s \geq y_i} \right)^2 ds \\ &= \frac{1}{n^3} \sum_{i,j,k} \int_{-\infty}^{+\infty} (\mathbb{1}_{s \geq y_j} - \mathbb{1}_{s \geq y_i})(\mathbb{1}_{s \geq y_k} - \mathbb{1}_{s \geq y_i}) ds \\ &= \frac{2}{n^3} \sum_{i < j < k} \int_{-\infty}^{+\infty} (\mathbb{1}_{s \geq y_{(j)}} - \mathbb{1}_{s \geq y_{(i)}})(\mathbb{1}_{s \geq y_{(k)}} - \mathbb{1}_{s \geq y_{(i)}}) ds \\ & \quad + \frac{2}{n^3} \sum_{j < i < k} \int_{-\infty}^{+\infty} (\mathbb{1}_{s \geq y_{(j)}} - \mathbb{1}_{s \geq y_{(i)}})(\mathbb{1}_{s \geq y_{(k)}} - \mathbb{1}_{s \geq y_{(i)}}) ds \\ & \quad + \frac{2}{n^3} \sum_{j < k < i} \int_{-\infty}^{+\infty} (\mathbb{1}_{s \geq y_{(j)}} - \mathbb{1}_{s \geq y_{(i)}})(\mathbb{1}_{s \geq y_{(k)}} - \mathbb{1}_{s \geq y_{(i)}}) ds \\ & \quad + \frac{2}{n^3} \sum_{j < i} \int_{-\infty}^{+\infty} (\mathbb{1}_{s \geq y_{(j)}} - \mathbb{1}_{s \geq y_{(i)}})^2 ds \\ &= \frac{2}{n^3} \sum_{i < j < k} (y_{(j)} - y_{(i)}) + 0 + \frac{2}{n^3} \sum_{j < k < i} (y_{(i)} - y_{(k)}) + \frac{2}{n^3} \sum_{j < i} (y_{(i)} - y_{(j)}) \\ &= \frac{2}{n^3} \sum_{i=1}^{n-2} \sum_{j=i+1}^{n-1} (n-j)(y_{(j)} - y_{(i)}) - \frac{2}{n^3} \sum_{j=1}^{n-2} \sum_{k=j+1}^{n-1} \sum_{i=k+1}^n (y_{(k)} - y_{(i)}) + \frac{2}{n^3} \sum_{i < j} (y_{(j)} - y_{(i)}) \\ &= \frac{2}{n^3} \sum_{i=1}^{n-1} \sum_{j=i+1}^n (n-j+1)(y_{(j)} - y_{(i)}) - \frac{2}{n^3} \sum_{j=1}^{n-2} \sum_{k=j+1}^{n-1} \sum_{i=k+1}^n (y_{(k)} - y_{(i)}) \end{aligned}$$

$$\begin{aligned}
&= -\frac{2}{n^3} \sum_{i=1}^{n-1} [n(n-i) - \frac{n(n-1)}{2} + \frac{i(i-1)}{2}] y_{(i)} + \frac{2}{n^3} \sum_{j=2}^n (n-j+1)(j-1) y_{(j)} \\
&\quad - \frac{2}{n^3} \sum_{i=3}^n \sum_{k=2}^{i-1} \sum_{j=1}^{k-1} (y_{(k)} - y_{(i)}) \\
&= -\frac{2}{n^3} \sum_{i=1}^{n-1} \frac{1}{2} (n-i)(n-i+1) y_{(i)} + \frac{2}{n^3} \sum_{j=2}^n (n-j+1)(j-1) y_{(j)} - \frac{2}{n^3} \sum_{i=3}^n \sum_{k=2}^{i-1} (k-1)(y_{(k)} - y_{(i)}) \\
&= -\frac{1}{n^3} \sum_{i=1}^{n-1} (n-i)(n-i+1) y_{(i)} + \frac{2}{n^3} \sum_{j=2}^n (n-j+1)(j-1) y_{(j)} \\
&\quad + \frac{2}{n^3} \sum_{i=3}^n \frac{(i-2)(i-1)}{2} y_{(i)} - \frac{2}{n^3} \sum_{k=2}^{n-1} (n-k)(k-1) y_{(k)} \\
&= -\frac{1}{n^3} \sum_{i=1}^{n-1} (n-i)(n-i+1) y_{(i)} + \frac{1}{n^3} \sum_{i=3}^n (i-2)(i-1) y_{(i)} + \frac{2}{n^3} \sum_{k=2}^n (k-1) y_{(k)} \\
&= -\frac{1}{n^3} \sum_{i=1}^n (n-i)(n-i+1) y_{(i)} + \frac{1}{n^3} \sum_{i=3}^n (i-2)(i-1) y_{(i)} + \frac{2}{n^3} \sum_{k=1}^n (k-1) y_{(k)} \\
&= \frac{1}{n^3} \sum_{i=1}^n [(i-2)(i-1) + 2(i-1) - (n-i)(n-i+1)] y_{(i)} \\
&= \frac{1}{n^3} \sum_{i=1}^n [i(i-1) - (n-i)(n-i+1)] y_{(i)} \\
&= \frac{1}{n^3} \sum_{i=1}^n (i-1)i(y_{(i)} - y_{(n-i+1)}).
\end{aligned}$$

We denote by $\mathbf{y}^{(n)}$ the vector of size n corresponding to the n first entries of the vector of observations \mathbf{y} (where we consider without loss of generality that elements in \mathbf{y} have been ordered considering the permutation sorting in increasing order $(x_{i,k})_{i:\mathbf{x}_i \in R_j}$ for some given node k and some feature j). From the previous computations we have

$$\frac{1}{n} \sum_{i=1}^n \text{CRPS}(\hat{F}, y_i) = \frac{1}{n^3} (h_{\uparrow}^{(n)} - h_{\downarrow}^{(n)}),$$

where

$$h_{\uparrow}^{(n)} := \sum_{i=1}^n (i-1)i y_{(i)}^{(n)} \quad \text{and} \quad h_{\downarrow}^{(n)} := \sum_{i=1}^n (i-1)i y_{(n-i+1)}^{(n)}.$$

In the following, we derive iterative formula for both $h_{\uparrow}^{(n)}$ and $h_{\downarrow}^{(n)}$.

Iterative formula for $h_{\uparrow}^{(n)}$.

$$\begin{aligned}
h_{\uparrow}^{(n+1)} - h_{\uparrow}^{(n)} &= \sum_{i=1}^{n+1} (i-1)i y_{(i)}^{(n+1)} - \sum_{i=1}^n (i-1)i y_{(i)}^{(n)} \\
&= \sum_{i=1}^{n+1} (i-1)i y_{(i)}^{(n+1)} - \sum_{i=1}^{r_{n+1}-1} (i-1)i y_{(i)}^{(n+1)} - \sum_{i=r_{n+1}}^n (i-1)i y_{(i+1)}^{(n+1)} \\
&= \sum_{i=1}^{n+1} (i-1)i y_{(i)}^{(n+1)} - \sum_{i=1}^{r_{n+1}-1} (i-1)i y_{(i)}^{(n+1)} - \sum_{i=r_{n+1}+1}^{n+1} (i-2)(i-1) y_{(i)}^{(n+1)}
\end{aligned}$$

$$\begin{aligned}
&= (r_{n+1} - 1)r_{n+1}y_{(r_{n+1})}^{(n+1)} + 2 \sum_{i=r_{n+1}+1}^{n+1} (i-1)y_{(i)}^{(n+1)} \\
&= [(r_{n+1} - 1)r_{n+1} - 2(r_{n+1} - 1)]y_{(r_{n+1})}^{(n+1)} + 2W^{(n+1)} \\
&\quad - 2 \sum_{i=1}^{r_{n+1}-1} iy_{(i)}^{(n+1)} - 2S^{(n+1)} + 2 \sum_{i=1}^{r_{n+1}-1} y_{(i)}^{(n+1)} \\
&= [(r_{n+1} - 1)r_{n+1} - 2(r_{n+1} - 1)]y_{(r_{n+1})}^{(n+1)} + 2W^{(n+1)} \\
&\quad - 2 \sum_{i=1}^{r_{n+1}-1} iy_{(i)}^{(n+1)} - 2S^{(n+1)} + 2S_{r_{n+1}-1}^{(n+1)}.
\end{aligned}$$

Iterative formula for $h_{\downarrow}^{(n)}$.

$$\begin{aligned}
h_{\downarrow}^{(n+1)} - h_{\downarrow}^{(n)} &= \sum_{i=1}^{n+1} (i-1)iy_{(n-i+2)}^{(n+1)} - \sum_{i=1}^n (i-1)iy_{(n-i+1)}^{(n)} \\
&= \sum_{i=1}^{n+1} (n-i+1)(n-i+2)y_{(i)}^{(n+1)} - \sum_{i=1}^n (n-i)(n-i+1)y_{(i)}^{(n)} \\
&= \sum_{i=1}^{n+1} (n-i+1)(n-i+2)y_{(i)}^{(n+1)} - \sum_{i=1}^{r_{n+1}-1} (n-i)(n-i+1)y_{(i)}^{(n+1)} \\
&\quad - \sum_{i=r_{n+1}}^n (n-i)(n-i+1)y_{(i+1)}^{(n+1)} \\
&= \sum_{i=1}^{n+1} (n-i+1)(n-i+2)y_{(i)}^{(n+1)} - \sum_{i=1}^{r_{n+1}-1} (n-i)(n-i+1)y_{(i)}^{(n+1)} \\
&\quad - \sum_{i=r_{n+1}+1}^{n+1} (n-i+1)(n-i+2)y_{(i)}^{(n+1)} \\
&= 2 \sum_{i=1}^{r_{n+1}-1} (n-i+1)y_{(i)}^{(n+1)} + (n-r_{n+1}+1)(n-r_{n+1}+2)y_{(r_{n+1})}^{(n+1)} \\
&= 2(n+1)S_{r_{n+1}-1}^{(n+1)} - 2 \sum_{i=1}^{r_{n+1}-1} iy_{(i)}^{(n+1)} + (n-r_{n+1}+1)(n-r_{n+1}+2)y_{(r_{n+1})}^{(n+1)}.
\end{aligned}$$

Conclusion. Using the previous computations, we obtain that

$$h_{\uparrow}^{(n+1)} - h_{\downarrow}^{(n+1)} = h_{\uparrow}^{(n)} - h_{\downarrow}^{(n)} + n[2r_{n+1} - 3 - n]y_{(r_{n+1})}^{(n+1)} + 2W^{(n+1)} - 2S^{(n+1)} - 2nS_{r_{n+1}-1}^{(n+1)}.$$

Noticing that $S_{r_{n+1}-1}^{(n+1)} = S_{r_{n+1}}^{(n+1)} - y_{n+1}$ concludes the proof.

C.2 Proof of Lemma 2

Querying $S^{(s)}$ in $\mathcal{O}(\log n)$ time. Let us recall that by construction, \mathcal{F} is at iteration s a Fenwick tree for the sequence $(1_{\sigma(i) \leq s} y_{\sigma(i)})_{i \in [n]}$. One can thus easily see that getting the sum of all elements in \mathcal{F} gives $S^{(s)} = \sum_{i=1}^s y_{(i)}^{(s)} = \sum_{i=1}^s y_i$. Indeed, up to ordering of the elements, the list $(1_{\sigma(i) \leq s} y_{\sigma(i)})_{i \in [n]}$ is equal to the one obtained by applying the permutation σ^{-1} namely to $(1_{i \leq s} y_i)_{i \in [n]}$ whose sum is equal to $S^{(s)}$. Hence, querying the sum of all elements of \mathcal{F} at iteration s gives $S^{(s)}$ and this operation requires $\mathcal{O}(\log n)$ time since \mathcal{F} is a Fenwick tree.

Querying $S_{r_s-1}^{(s)}$ in $\mathcal{O}(\log n)$ time. Let us now prove that querying the sum of all elements in \mathcal{F} from position 1 to $\sigma^{-1}(s)$ at iteration s is equal to $S_{r_s}^{(s)}$. This will prove that $S_{r_s}^{(s)}$ can be obtained in $\mathcal{O}(\log n)$ time since \mathcal{F} is a Fenwick tree. One can then get $S_{r_s-1}^{(s)}$ using that $y_{(r_s)}^{(s)} = y_s$ and thus that

$$S_{r_s-1}^{(s)} = S_{r_s}^{(s)} - y_s.$$

Indeed, $S_{r_s-1}^{(s)} = \sum_{i=1}^{r_s-1} y_{(i)}^{(s)}$ where r_s is the position of insertion of y_s in the non-decreasing sorted version of the list $\mathbf{y}^{(s-1)}$.

Since $y_{(r_s)}^{(s)} = y_s$, the list $(y_{(1)}^{(s)}, \dots, y_{(r_s)}^{(s)})$ exactly corresponds to all the elements in (y_1, \dots, y_s) smaller than y_s i.e. to the list of all y_k for $k \leq s$ such that $\sigma^{-1}(k) \leq \sigma^{-1}(s)$. We deduce that

$$S_{r_s}^{(s)} = \sum_{i=1}^{r_s} y_{(i)}^{(s)} = \sum_{i=1}^s 1_{\sigma^{-1}(i) \leq \sigma^{-1}(s)} y_i = \sum_{j \in \{\sigma^{-1}(k) | k \in [s]\}} 1_{j \leq \sigma^{-1}(s)} y_{\sigma(j)} = \sum_{j=1}^{\sigma^{-1}(s)} 1_{\sigma(j) \leq s} y_{\sigma(j)}, \quad (8)$$

where in the penultimate equality we made the change of variable $i = \sigma(j)$ and where in the last equality we used that

$$\{\sigma^{-1}(k) | k \in [s], \sigma^{-1}(k) \leq \sigma^{-1}(s)\} = \{j | j \in [\sigma^{-1}(s)], \sigma(j) \leq s\}.$$

Since \mathcal{F} is at iteration s a Fenwick tree for the sequence $(1_{\sigma(i) \leq s} y_{\sigma(i)})_{i \in [n]}$, we deduce from Eq.(8) that querying the sum of elements from position 1 to $\sigma^{-1}(s)$ in \mathcal{F} gives $S_{r_s}^{(s)}$.

As a remark, one can notice that a direct consequence of this result is that querying the sum of all elements from position 1 to $\sigma^{-1}(s+1)$ at iteration s from \mathcal{F} gives $S_{r_{s+1}-1}^{(s)}$.

Getting $W^{(s+1)}$ in constant time given $W^{(s)}$, $S^{(s)}$ and $S_{r_{s+1}-1}^{(s+1)}$. The total rank-weighted sum $W^{(s)}$ can be efficiently tracked along the iterative process using the formula

$$W^{(s+1)} = W^{(s)} + r_{s+1} y_{s+1} + \sum_{i=r_{s+1}}^s y_{(i)}^{(s)} = W^{(s)} + r_{s+1} y_{s+1} + S^{(s)} - S_{r_{s+1}-1}^{(s)}, \quad (9)$$

where

$$S_{r_{s+1}-1}^{(s)} = S_{r_{s+1}-1}^{(s+1)},$$

since r_{s+1} is the position of insertion of y_{s+1} in the list $(y_{(1)}^{(s)}, \dots, y_{(s)}^{(s)})$.

D Unbiased estimate of entropies using leave-one-out

D.1 LOO for PMQRT

We propose using a leave-one-out method to obtain an unbiased estimate of the information gain used to build the PQRT or PMQRT. In the following, we show that such LOO estimate of the entropy associated with a pinball loss ℓ_τ with data $\mathbf{y} = (y_1, \dots, y_n)$ can be computed efficiently.

Let us denote by \mathcal{H}_n the entropy of the sequence \mathbf{y} and by $\mathcal{H}_{n,LOO}$ the leave-one-out estimate of the entropy of \mathbf{y} for the pinball loss ℓ_τ , namely

$$\mathcal{H}_n = \frac{1}{n} \sum_{i=1}^n \ell_\tau(y_i, \hat{q}_\tau), \quad \mathcal{H}_{n,LOO} = \frac{1}{n} \sum_{i=1}^n \ell_\tau(y_i, \hat{q}_\tau^{-i}),$$

where \hat{q}_τ (resp. \hat{q}_τ^{-i}) is the empirical quantile of order τ of the sequence \mathbf{y} (resp. $\mathbf{y}^{-i} := (y_1, \dots, y_{i-1}, y_{i+1}, \dots, y_n)$).

Let us consider a permutation σ sorting the sequence \mathbf{y} by increasing order. We further denote $r_i := \sigma^{-1}(i)$ which corresponds to the position in the sorted list of the element y_i . Defining $r^- := \lceil \tau(n-1) \rceil$ and $r^* := \lceil n\tau \rceil$, we can distinguish two possible cases:

- If $r^- = r^*$:
 - If $r_i > r^-$: $\ell_\tau(y_i, \hat{q}_\tau^{-i}) = \ell_\tau(y_i, \hat{q}_\tau) = \tau(y_i - y_{(r^*)})$.
 - Else: $\ell_\tau(y_i, \hat{q}_\tau^{-i}) = (1 - \tau)(y_{(r^*+1)} - y_i)$.

Hence:

$$\begin{aligned}\mathcal{H}_{n,LOO} &= \mathcal{H}_n - (1 - \tau) \sum_{i|r_i \leq r^*} (y_{(r^*)} - y_i) + (1 - \tau) \sum_{i|r_i \leq r^*} (y_{(r^*+1)} - y_i) \\ &= \mathcal{H}_n + (1 - \tau)r^*(y_{(r^*+1)} - y_{(r^*)}).\end{aligned}$$

- Else (i.e. if $r^- + 1 = r^*$):
 - If $r_i > r^-$: $\ell_\tau(y_i, \hat{q}_\tau^{-i}) = \ell_\tau(y_i, y_{(r^*-1)}) = \tau(y_i - y_{(r^*-1)})$.
 - Else: $\ell_\tau(y_i, \hat{q}_\tau^{-i}) = (1 - \tau)(y_{(r^*)} - y_i)$.

Hence:

$$\begin{aligned}\mathcal{H}_{n,LOO} &= \mathcal{H}_n - \tau \sum_{i|r_i \leq r^*} (y_i - y_{(r^*)}) + \tau \sum_{i|r_i \leq r^*} (y_i - y_{(r^*-1)}) \\ &= \mathcal{H}_n + \tau(n - r^* + 1)(y_{(r^*)} - y_{(r^*-1)}).\end{aligned}$$

All quantities $y_{(r^*-1)}$, $y_{(r^*)}$ and $y_{(r^*+1)}$ can be queried in $\mathcal{O}(\log(n))$ time using the min-max heap structures used to train PMQRT (or PQRT). Overall, a node split using or not these LOO estimates of entropies is performed in $\mathcal{O}(pn \log(n))$ time where p is the number of features and n is the number of data points in the leaf. Therefore, no additional cost is induced by using LOO.

Figure 7 illustrates on a numerical example the difference on the estimated conditional quantiles when learning PMQRTs using or not without.

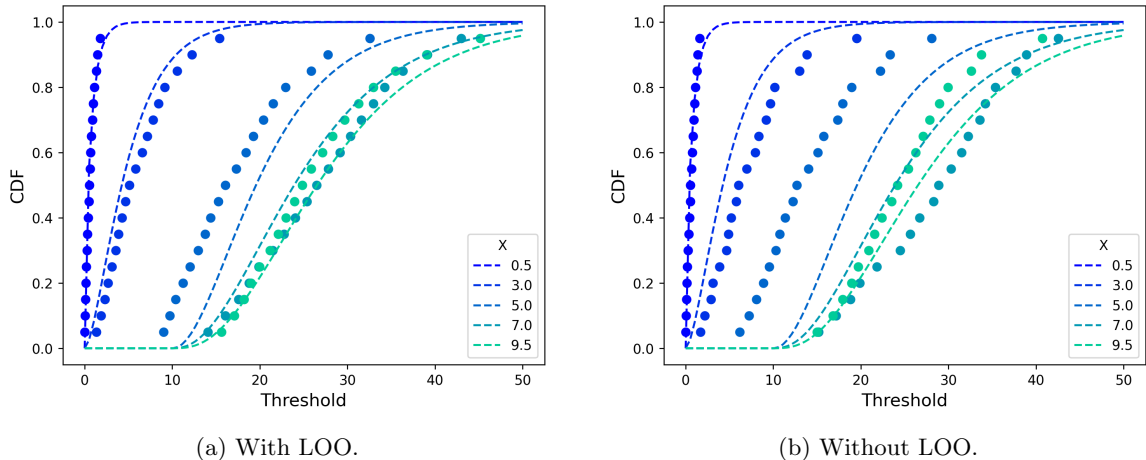


Figure 7: Estimation of the conditional CDF of y given x with PMQRF with 100 on a sample of size $n = 600$ simulated from the distribution in Eq.(Gamma). The true conditional CDFs (smooth dashed lines) are compared to the quantile estimates obtained from PMQRF (dots).

D.2 LOO for CRPS-RT

It is noteworthy that using leave-one-out to obtain an unbiased estimate of the information gain at each node for determining the best split is very simple. In fact, the computations presented below show that the leave-one-out estimate of the information gain can be efficiently derived by appropriately scaling the standard empirical entropies.

Denoting by \hat{F}^{-i} the empirical CDF obtained from the sequence $(y_1, \dots, y_{i-1}, y_{i+1}, \dots, y_n)$, we have

$$\begin{aligned}
& \frac{1}{n} \sum_{i=1}^n \text{CRPS}(\hat{F}^{-i}, y_i) \\
&= \frac{1}{n} \sum_{i=1}^n \int_{-\infty}^{+\infty} (\hat{F}^{-i}(s) - \mathbb{1}_{s \geq y_i})^2 ds \\
&= \frac{1}{n} \sum_{i=1}^n \int_{-\infty}^{+\infty} \left(\frac{1}{n-1} \sum_{j \neq i} \mathbb{1}_{s \geq y_j} - \mathbb{1}_{s \geq y_i} \right)^2 ds \\
&= \frac{1}{n(n-1)^2} \sum_{i=1}^n \sum_{j \neq i} \sum_{k \neq i} \int_{-\infty}^{+\infty} (\mathbb{1}_{s \geq y_j} - \mathbb{1}_{s \geq y_i})(\mathbb{1}_{s \geq y_k} - \mathbb{1}_{s \geq y_i}) ds \\
&= \frac{1}{n(n-1)^2} \sum_{i=1}^n \sum_{j=1}^n \sum_{k=1}^n \int_{-\infty}^{+\infty} (\mathbb{1}_{s \geq y_j} - \mathbb{1}_{s \geq y_i})(\mathbb{1}_{s \geq y_k} - \mathbb{1}_{s \geq y_i}) ds \\
&= \frac{n^2}{(n-1)^2} \left(\frac{1}{n} \sum_{i=1}^n \text{CRPS}(\hat{F}, y_i) \right).
\end{aligned}$$

References

- [AR15] Sachinthaka Abeywardana and Fabio Ramos. Variational inference for nonparametric Bayesian quantile regression. *Proceedings of the AAAI Conference on Artificial Intelligence*, 29(1), Feb. 2015.
- [BFSO84] L. Breiman, J. Friedman, C.J. Stone, and R.A. Olshen. *Classification and Regression Trees*. Taylor & Francis, 1984.
- [BG21] Jonas R. Brehmer and Tilmann Gneiting. Scoring interval forecasts: Equal-tailed, shortest, and modal interval. *Bernoulli*, 27(3), May 2021.
- [BKV15] Harish S Bhat, Nitesh Kumar, and Garnet J Vaz. Towards scalable quantile regression trees. In *2015 IEEE International Conference on Big Data (Big Data)*, pages 53–60. IEEE, 2015.
- [Bre17] Leo Breiman. *Classification and regression trees*. Routledge, 2017.
- [BRGR21] Johannes Bracher, Evan L. Ray, Tilmann Gneiting, and Nicholas G. Reich. Evaluating epidemic forecasts in an interval format. *PLOS Computational Biology*, 17(2):1–15, 02 2021.
- [BS21] Han Bao and Masashi Sugiyama. Fenchel-Young losses with skewed entropies for class-posterior probability estimation. In *International Conference on Artificial Intelligence and Statistics*, pages 1648–1656. PMLR, 2021.
- [Can11] Alex J. Cannon. Quantile regression neural networks: Implementation in r and application to precipitation downscaling. *Computers & Geosciences*, 37(9):1277–1284, 2011.
- [CC21] Enrico Camporeale and Algo Carè. ACCRUE: Accurate and reliable uncertainty estimate in deterministic models. *International Journal for Uncertainty Quantification*, 11(4), 2021.
- [CWZ21] Victor Chernozhukov, Kaspar Wüthrich, and Yinchu Zhu. Distributional conformal prediction. *Proceedings of the National Academy of Sciences*, 118(48):e2107794118, 2021.
- [DeG62] M. H. DeGroot. Uncertainty, Information, and Sequential Experiments. *The Annals of Mathematical Statistics*, 33(2):404 – 419, 1962.
- [DPP07] David B Dunson, Natesh Pillai, and Ju-Hyun Park. Bayesian density regression. *Journal of the Royal Statistical Society Series B: Statistical Methodology*, 69(2):163–183, 2007.

[EM04] Robert F Engle and Simone Manganelli. Caviar. *Journal of Business & Economic Statistics*, 22(4):367–381, 2004.

[GD04] Peter D. Grünwald and A. Philip Dawid. Game theory, maximum entropy, minimum discrepancy and robust Bayesian decision theory. *The Annals of Statistics*, 32(4):1367 – 1433, 2004.

[GKR22] Chirag Gupta, Arun K Kuchibhotla, and Aaditya Ramdas. Nested conformal prediction and quantile out-of-bag ensemble methods. *Pattern Recognition*, 127:108496, 2022.

[GL07] Bettina Grün and Friedrich Leisch. Fitting finite mixtures of generalized linear regressions in R. *Computational Statistics & Data Analysis*, 51(11):5247–5252, 2007.

[GR07] Tilmann Gneiting and Adrian E Raftery. Strictly proper scoring rules, prediction, and estimation. *Journal of the American statistical Association*, 102(477):359–378, 2007.

[HH13] S. Halim and F. Halim. *Competitive Programming 3: The New Lower Bound of Programming Contests*. Number vol. 3. Lulu.com, 2013.

[HJA20] Jonathan Ho, Ajay Jain, and Pieter Abbeel. Denoising diffusion probabilistic models. *Advances in neural information processing systems*, 33:6840–6851, 2020.

[HV99] James T. Hamilton and W Viscusi. Are risk regulators rational? evidence from hazardous waste cleanup decisions. *American Economic Review*, 89(4):1010–1027, 1999.

[JKL17] Alexander Jordan, Fabian Krüger, and Sebastian Lerch. Evaluating probabilistic forecasts with scoringRules. *arXiv preprint arXiv:1709.04743*, 2017.

[JOM⁺16] Romain Juban, Henrik Ohlsson, Mehdi Maasoumy, Louis Poirier, and J Zico Kolter. A multiple quantile regression approach to the wind, solar, and price tracks of GEFCom2014. *International Journal of Forecasting*, 32(3):1094–1102, 2016.

[KBJ78] Roger Koenker and Gilbert Bassett Jr. Regression quantiles. *Econometrica: journal of the Econometric Society*, pages 33–50, 1978.

[KPB20] Ivan Kobyzev, Simon JD Prince, and Marcus A Brubaker. Normalizing flows: An introduction and review of current methods. *IEEE transactions on pattern analysis and machine intelligence*, 43(11):3964–3979, 2020.

[KS22] Karunarathna B Kulasekera and Chathura Siriwardhana. Quantiles based personalized treatment selection for multivariate outcomes and multiple treatments. *Statistics in medicine*, 41(15):2695–2710, 2022.

[KSS23] Thomas Kneib, Alexander Silbersdorff, and Benjamin Säfken. Rage against the mean – a review of distributional regression approaches. *Econometrics and Statistics*, 26:99–123, 2023.

[LW09] Yufeng Liu and Yichao Wu. Stepwise multiple quantile regression estimation using non-crossing constraints. *Statistics and its Interface*, 2(3):299–310, 2009.

[MR06] Nicolai Meinshausen and Greg Ridgeway. Quantile regression forests. *Journal of machine learning research*, 7(6), 2006.

[MS04] Dinesh P Mehta and Sartaj Sahni. *Handbook of data structures and applications*. Chapman and Hall/CRC, 2004.

[MSP22] Santiago Mazuelas, Yuan Shen, and Aritz Pérez. Generalized maximum entropy for supervised classification. *IEEE Transactions on Information Theory*, 68(4):2530–2550, 2022.

[NR73] J. Nievergelt and E. M. Reingold. Binary search trees of bounded balance. *SIAM Journal on Computing*, 2(1):33–43, 1973.

[RBL⁺22] Robin Rombach, Andreas Blattmann, Dominik Lorenz, Patrick Esser, and Björn Ommer. High-resolution image synthesis with latent diffusion models. In *Proceedings of the IEEE/CVF conference on computer vision and pattern recognition*, pages 10684–10695, 2022.

[Reg17] Quantile Regression. *Handbook of quantile regression*. CRC Press: Boca Raton, FL, USA, 2017.

[RPC19] Yaniv Romano, Evan Patterson, and Emmanuel Candès. Conformalized quantile regression. *Advances in neural information processing systems*, 32, 2019.

[RS05] R. A. Rigby and D. M. Stasinopoulos. Generalized Additive Models for Location, Scale and Shape. *Journal of the Royal Statistical Society Series C: Applied Statistics*, 54(3):507–554, 04 2005.

[SC20] Matteo Sesia and Emmanuel J Candès. A comparison of some conformal quantile regression methods. *Stat*, 9(1):e261, 2020.

[SM24] Xinwei Shen and Nicolai Meinshausen. Engression: Extrapolation through the lens of distributional regression, 2024.

[TCM⁺10] Paul Thompson, Yuzhi Cai, Rana Moyeed, Dominic Reeve, and Julian Stander. Bayesian nonparametric quantile regression using splines. *Computational Statistics & Data Analysis*, 54(4):1138–1150, 2010.

[TLSS06] Ichiro Takeuchi, Quoc V. Le, Timothy D. Sears, and Alexander J. Smola. Nonparametric quantile estimation. *Journal of Machine Learning Research*, 7:1231 – 1264, 2006. Cited by: 319.

[TPFG20] Léonard Torossian, Victor Picheny, Robert Faivre, and Aurélien Garivier. A review on quantile regression for stochastic computer experiments. *Reliability Engineering & System Safety*, 201:106858, 2020.

[Xu20] Aolin Xu. Continuity of generalized entropy. In *2020 IEEE International Symposium on Information Theory (ISIT)*, pages 2246–2251, 2020.

[ZY08] Hui Zou and Ming Yuan. Regularized simultaneous model selection in multiple quantiles regression. *Computational Statistics & Data Analysis*, 52(12):5296–5304, 2008.